


Article

Response of Typical Tree Species Sap Flow to Environmental Factors in the Hilly Areas of Haihe River Basin, China

Shuying Han ^{1,2}, Qingming Wang ^{1,2,3,*}, Yong Zhao ^{1,2} , Jiaqi Zhai ^{1,2}, Xiang Wang ⁴, Yan Hao ⁵, Linghui Li ^{1,2}, Xing Li ^{1,2}, Haihong Li ^{1,2} and Jiansheng Cao ⁶

- ¹ China Institute of Water Resources and Hydropower Research, Beijing 100038, China; hsy20221122@163.com (S.H.); zhaoyong@iwhr.com (Y.Z.); jiaqizhai@163.com (J.Z.); lilingshuihill@163.com (L.L.); lixingiwhr@163.com (X.L.); lihh@iwhr.com (H.L.)
- ² State Key Laboratory of Simulation and Regulation of Water Cycle in River Basin, Beijing 100038, China
- ³ Key Laboratory of Water Safety for Beijing-Tianjin-Hebei Region of Ministry of Water Resources, Beijing 100038, China
- ⁴ School of Water Conservancy and Transportation, Zhengzhou University, Zhengzhou 450001, China; sky15227506812@163.com
- ⁵ School of Civil Engineering, Shijiazhuang Tiedao University, Shijiazhuang 050043, China; haoyan147258@gmail.com
- ⁶ Key Laboratory of Agricultural Water Resources, Center for Agricultural Resources Research, Institute of Genetics and Developmental Biology, Chinese Academy of Sciences, Shijiazhuang 050021, China; caojs@sjziam.ac.cn
- * Correspondence: wangqm@iwhr.com; Tel.: +86-138-1002-4452

Abstract: Understanding developments in the trunk sap flow of prevalent tree species within the hilly areas of the Haihe River basin is imperative for ecosystem conservation. Nevertheless, the changes in sap flow of local trees and their response to environmental factors remain elusive. This study focuses on seven dominant tree species in the hilly area of the Haihe River basin and analyzed the relationship between tree sap flow rate and environmental factors at different time scales (hourly and daily). Our findings suggested: (1) Regardless of the time scale, total solar irradiance played a primary role in influencing sap flow rate. Conversely, as the time scale grew, the associations between most soil factors and sap flow rate enhanced, while those with meteorological factors declined. Notably, soil temperature exerted a more profound influence on sap flow rate than soil moisture and conductivity. (2) At the hourly scale, the sap flow rate of each species had a lag effect of 1–2 h with vapour pressure deficit, relative humidity and temperature, and 1 h or no lag effect with total solar irradiance and wind speed. (3) The response model of sap flow rate and environmental factors showed that, except for *Pinus tabuliformis* Carr., other tree species fit well at various time scales ($R^2 \geq 0.59$). As the time scale of most tree species increased from hourly scale to daily scale, the fit gradually weakened. Concurrently, considering the time-lag effect, the accuracy of the model has been improved, and the fitting accuracy of *Koeleruteria paniculata* Laxm. and *Pinus tabuliformis* Carr. has been significantly improved.

Keywords: sap flow rate; meteorological factors; soil factors; different time scales; time lag



Citation: Han, S.; Wang, Q.; Zhao, Y.; Zhai, J.; Wang, X.; Hao, Y.; Li, L.; Li, X.; Li, H.; Cao, J. Response of Typical Tree Species Sap Flow to Environmental Factors in the Hilly Areas of Haihe River Basin, China. *Forests* **2024**, *15*, 294. <https://doi.org/10.3390/f15020294>

Academic Editors: Nadezhda Nadezhkina, Benye Xi and Jie Duan

Received: 20 December 2023

Revised: 26 January 2024

Accepted: 1 February 2024

Published: 3 February 2024



Copyright: © 2024 by the authors. Licensee MDPI, Basel, Switzerland. This article is an open access article distributed under the terms and conditions of the Creative Commons Attribution (CC BY) license (<https://creativecommons.org/licenses/by/4.0/>).

1. Introduction

Transpiration is the process by which plants absorb soil water through their roots, pass it through their xylem to their leaves, and release it into the atmosphere [1,2]. Water consumed by transpiration accounts for more than 90% of the absorbed soil water [3]. Transpiration is a key link in water transport in the soil–plant–atmosphere continuum and plays a key role in regulating local climate, affecting soil water content and runoff [4–6]. Therefore, understanding the water consumption pattern of plant transpiration and the mechanism that controls its dynamic changes is greatly significant for studying the role

of plant transpiration in forest water balance and accurately estimating and predicting large-scale vegetation water and carbon fluxes [7,8].

More than 99.8% of plant transpiration originates from sap flow, and the sap flow rate (V) can therefore accurately describe the water consumption process of individual trees [1,2]. Common methods for measuring sap flow include the heat pulse method [9,10], stem segment heat balance method [11,12], thermal diffusion probe method [13], and heat field deformation method [14], of which the thermal diffusion probe method for measuring sap flow is the most commonly used, because of its convenient operation and high measurement accuracy [13]. A large number of studies based on experiments have shown that the transpiration of different tree species is affected by the physiological structure of plants and environmental factors. The physiological structure of plants (such as leaf area index, sapwood, crown width, and phenology) determines their potential for transpiration [15–18]. Environmental factors that impact V include meteorological factors, such as temperature (T_a), total solar irradiance (TSI), relative humidity (RH), vapour pressure deficit (VPD), wind speed (WS), and precipitation (P), which determine the instantaneous changes in transpiration and are the main driving force of canopy transpiration [19–24], and soil factors, such as soil moisture content and soil temperature, which determine the peak and total transpiration of plants [25–27]. In particular, when soil moisture is limited, the hydraulic resistance of the soil and roots increases, leading to delayed water transport and stomatal closure [28,29]. However, there is still significant uncertainty regarding the interactions between factors that affect vegetation transpiration and their impact on sap flow. In addition, the differences in regions and tree species lead to significant uncertainty in transpiration characteristics and the impact of environmental factors. For instance, the characteristics of tree transpiration in response to environmental factors are influenced by the trees' water use strategies, which include isohydric and anisohydric behaviors. The sap flow of anisohydric trees like European beech is not affected by soil water content and is purely driven by atmospheric evaporative demand [30,31]. But the sap flow of isohydric trees like Norway spruce is strongly affected by soil water content, as they close their stomata early in drought events [32,33]. It is necessary to establish an accurate and reliable model to describe the relationship between sap flow and the different influencing factors. At the same time, researching the transpiration patterns of different regions and tree species and their response to environmental factors is of great significance for efforts to improve the accuracy of local transpiration estimation.

Several studies have found that the response of sap flow to environmental factors has a significant timescale effect. This includes two aspects: (1) The main controlling factors that affect sap flow differ at different time scales; multiple studies have proven that TSI and VPD are important factors controlling V at hourly scales [34–36]; at daily and monthly scales, soil moisture, soil temperature, and leaf phenology play more important roles [37–40]. (2) The time lag effect of sap flow is defined as the time difference between the peak value of sap flow rate and the peak value of driving factors such as solar radiation and VPD, which exist for between several minutes and several hours [41]. The lag between sap flow and environmental factors is often considered to be a self-protection mechanism for plants to avoid dehydration [42]. Previous studies have shown that, when interpolating or simulating tree trunk sap flow, the failure to consider the time lag effect between sap flow and environmental factors can lead to an error of up to 30% occurring between the calculated value and the actual value [43,44]. When using models to simulate tree trunk sap flow, considering phenological indices and time lag effects can improve the accuracy of sap flow calculation [45]. Conducting the time lag effect of plant sap flow on environmental factors can help establish more accurate regional water consumption models and is of great significance for a deeper understanding of changes in tree transpiration water consumption.

The hilly areas of the Haihe River basin in China are important soil erosion areas. In recent years, with the policy of prohibiting tree logging in mountainous areas and implementing afforestation, vegetation restoration in these areas has become significant [46]. The large-scale reconstruction of local vegetation has led to an increase in transpiration,

followed by a significant decrease in runoff, which has altered the characteristics of regional water circulation [47]. The transpiration characteristics of local vegetation have gradually received widespread attention [48–50]. Understanding the water use of vegetation in the region will provide a theoretical basis for the utilisation of scarce water resources in the local area, as well as for the selection and rational planning of afforestation tree species in arid and semi-arid mountainous areas.

This study focused on seven dominant tree species in the hilly areas of the Haihe River basin. Based on the measured V data obtained from 1 May to 31 October 2022 and environmental variables (meteorological and soil factors) taken during the same period, the variation characteristics of V and its response to environmental factors at different timescales were explored. Specifically, our research objectives were to determine: (1) the variation characteristics of V at different timescales, including hourly and daily scales; (2) the relationship between V and environmental factors at different timescales by using Pearson correlation, random forest, and stepwise regression R^2 ; and (3) a regression model considering time lag effect was established for V and environmental factors, and the differences in fitting effects between regression models, both with and without time delay, were compared.

2. Materials and Methods

2.1. Study Area

Figure 1 showed the location of the study area. It was located in the Taihang Mountain Ecological Experimental Station, Chinese Academy of Sciences, which is in Yuanshi County, Hebei Province, China ($114^{\circ}15'20''$ E, $37^{\circ}54'17''$ N). The elevation of the area is approximately 323–404 m, belonging to the shallow mountainous area of the Haihe River basin. The sub-basin area where the station is located is approximately 15.9 km². The region has a warm temperate semi-arid and semi-humid mountain climate, with an average annual precipitation of 500 mm and an average annual temperature of 12.6 °C. The main tree species include *Populus hopeiensis*, *Robinia pseudoacacia*, *Pinus tabuliformis* Carr., and *Juglans regia*.

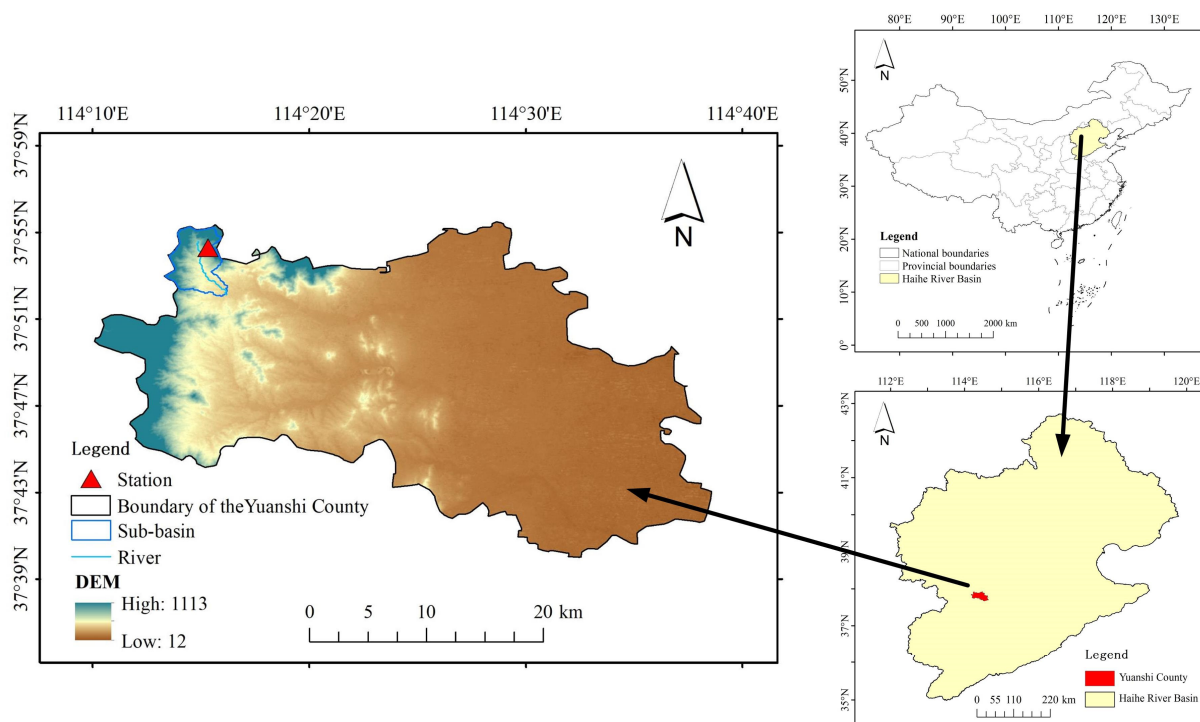


Figure 1. Location of the study area.

2.2. Layout of Monitoring Points

Based on the terrain characteristics and tree types of the study area, five monitoring points (A–E) were established in September 2021, and seven typical trees were selected for measurement. A total of 2–4 trees were selected for each tree type for sap flow monitoring. Finally, two trees of each type, with similar growth, straight trunks and no disease, were selected for analysis. In addition, 10 soil profiles were deployed at three sample sites (A, C, and D) to monitor soil parameters, including soil moisture content (W), soil conductivity (E), and soil temperature (T). The spatial distribution and basic information of the sample points are shown in Figure 2 and Table 1, respectively.

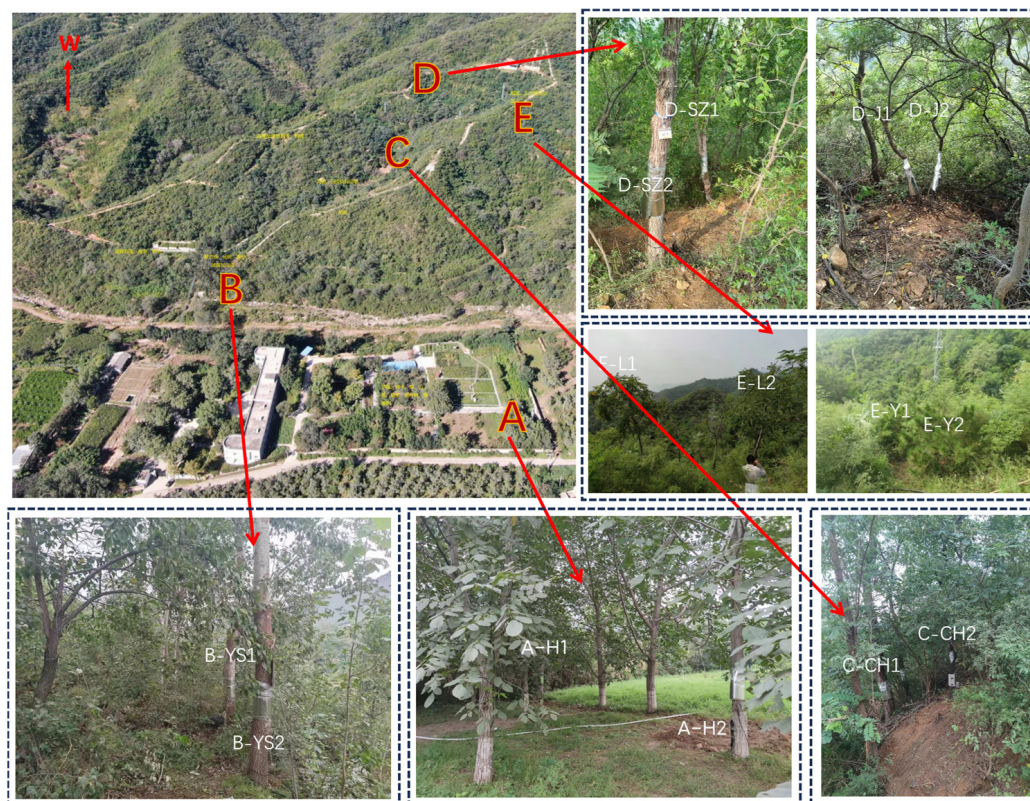


Figure 2. Spatial distribution of sample points. A–E represents monitoring points. A–H1 and A–H2 represent *Juglans regia* at point A. B–YS1 and B–YS2 represent *Populus hopeiensis* at point B. C–CH1 and C–CH2 represent *Robinia pseudoacacia* at point C. D–SZ1 and D–SZ2 represent *Ziziphus jujuba* Mill. var. *spinosa* (Bunge) Hu ex H. F. Chow. at point D. D–J1 and D–J2 represent *Vitex negundo* L. var. *heterophylla* (Franch.) Rehd. at point D. E–L1 and E–L2 represent *Koelreuteria paniculata* Laxm. at point E. E–Y1 and E–Y2 represent *Pinus tabuliformis* Carr. at point E.

2.3. Determination of Sap Flow

According to literature reviews, the starting and ending periods of the plant growth season in the study area are roughly from mid April to early November [51,52]. Therefore, we define May to October as the growth period of trees, which we use to study the relationship between trunk sap flow rate and environmental factors during this period. Thermal dissipation probes (TDP, Dynamax Inc., Houston, TX, USA) were installed on the trunk of the sample tree, 1.3 m above the ground for sap flow monitoring [13]. To avoid the effect of solar radiation on the probe temperature, the probe was installed on the north side of the tree trunk and wrapped in tin foil. Waterproof tape was used to seal the upper boundary of the tin foil and the junction of the trunk, to prevent damage to the probe due to precipitation. A CR1000 data collector (Campbell Scientific Inc., North Logan, UT, USA)

was used to read the data every 30 s and to record the average value every 10 min. The sap flow rate (V) was obtained according to the Granier [13] empirical formula:

$$V = 0.0119 \times \left(\frac{\Delta T_{Max} - \Delta T}{\Delta T} \right)^{1.231} \quad (1)$$

where V (cm/s) is the sap flow rate, ΔT ($^{\circ}\text{C}$) is the temperature difference between the heating probe and the reference probe, and ΔT_{Max} ($^{\circ}\text{C}$) is the maximum temperature difference, which is generally the temperature difference in the early morning when the sap flow rate is close to zero.

Table 1. Parameter information of the sample point.

Sample Point	Tree Name	Tree Number	H ¹ m	DBH ² cm	Anatomical Structure of Xylem	As cm ²	Soil Profile ³
A	<i>Juglans regia</i> (H) ⁴	A-H1, A-H2	10.5	18.3	Semi-ring porous to diffuse-porous	250.9	5 layers (0–100 cm)
B	<i>Populus hopeiensis</i> (YS)	B-YS1, B-YS2	20.5	29.7	Diffuse-porous	253.1	/
C	<i>Robinia pseudoacacia</i> (CH)	C-CH1, C-CH2	10	21.4	Ring-porous	133	3 layers (0–60 cm)
D	<i>Ziziphus jujuba</i> Mill. var. <i>spinosa</i> (Bunge) Hu ex H. F. Chow. (SZ)	D-SZ1, D-SZ2	9.8	13.8	Diffuse-porous	127.2	2 layers (0–40 cm)
	<i>Vitex negundo</i> L. var. <i>heterophylla</i> (Franch.) Rehd. (J)	D-J1, D-J2	2.7	6.2	Ring-porous	16.1	
E	<i>Koeleruteria paniculata</i> Laxm. (L)	E-L1, E-L2	3.5	6.5	Ring-porous	22.5	/
	<i>Pinus tabuliformis</i> Carr. (Y)	E-Y1, E-Y2	1.3	6.2	Ring-porous	18.1	
Total							10

¹ H is the average tree height. ² DBH is the average diameter at breast height of trees. ³ The soil profile is set at intervals of 20 cm. ⁴ The contents in parentheses at the end of the tree name are short names.

The direct use of Granier's empirical formula will be affected by errors. Many studies have confirmed that the direct use of the empirical formula will, if parameters are not corrected, result in the overestimation or underestimation of the actual sap flow to varying degrees [53,54]. However, in this study, more attention was paid to the trend of sap flow rate at hourly and daily scales, as well as its relationship with environmental factors, rather than studying the absolute value of tree transpiration. Therefore, it would not affect the results.

2.4. Determination of Environmental Factors

2.4.1. Meteorological Factors

An automatic small weather station was installed in the study area to synchronously monitor meteorological factors and record data once per hour. The monitoring indicators include temperature (T_a , $^{\circ}\text{C}$), relative humidity (RH , %), total solar irradiance (TSI , MJ/m^2), wind speed (WS , m/s), and precipitation (P , mm). The vapour pressure deficit (VPD , kPa), which reflects the degree of dryness of the air and largely controls physiological processes such as vegetation transpiration, was calculated using T_a and RH , as follows [55]:

$$VPD = a \exp\left(\frac{bT_a}{T_a + c}\right)(1 - RH) \quad (2)$$

where VPD is the water vapor pressure deficit (kPa), T_a is the temperature ($^{\circ}\text{C}$), and RH is the relative humidity (%). a , b , and c are constants with values of 0.611, 17.502, and 240.97, respectively.

2.4.2. Soil Factors

The soil moisture monitoring profile is set at a horizontal distance of 0.5–1m from the tree roots. Soil moisture content, temperature, and conductivity were measured. Probes were embedded at different depths (10 cm intervals) in the sample site, the data acquisition interval was set to 10 min, and the measurement time was synchronised with TDP.

2.5. Data Processing

MATLAB 2021 was used to convert the original measured temperature difference data into sap flow rate data. Pearson's correlation analysis was used to quantify the correlation between V and environmental factors, at both hourly and daily scales. The relative importance of environmental factors to V was assessed using stepwise regression, R^2 variation, and random forest regression. The time-lag effect between the environmental factors and V was studied based on a time-dislocation analysis. A response model of V at hourly and daily scales was constructed based on a stepwise regression model. The difference in the fitting effect between the models, with and without a time delay, was then analysed on an hourly scale. Origin 2021 was used to complete all the resulting graphs in this study.

3. Results

3.1. Dynamic Changes in Environmental Factors

3.1.1. Meteorological Factors

According to the observational data (Figure 3), during the study period, T_a , RH , TSI , and P showed trends of first increasing and then decreasing, whereas WS and VPD first decreased and then increased. T_a ranged from 8.3 to 32.42 $^{\circ}\text{C}$, with an average of 22 $^{\circ}\text{C}$. RH ranged from 20.47–100%, with an average of 70.06%. The TSI ranged from 0.32 to 8.85 $\text{MJ}/(\text{m}^2\cdot\text{d})$, with an average of 5.2 $\text{MJ}/(\text{m}^2\cdot\text{d})$. The wind speed was 0–0.37 m/s, with an average of 0.37 m/s. The cumulative rainfall during the growing season was 467.87 mm and was mostly concentrated from June to August, accounting for 77.5% of the total rainfall of the growing season. The highest rainfall was recorded in August, (147.07 mm). Summer was the most active period of the hydrological cycle in the mountainous area, during which rainfall was more concentrated and evaporation was more intense. The daily average VPD during the growing season was 0.83 kPa, and when rainfall events occurred, the VPD significantly decreased.

3.1.2. Dynamic Changes of Soil Factors

The monitoring data (Figure 4) showed that the soil water content of each layer was relatively stable and exhibited a slow decreasing trend under dry and no-rain conditions. When precipitation events occurred, the soil moisture content and conductivity from 0 to 60 cm fluctuated significantly, while that from 60 cm and greater did not. The soil temperature at the sampling points during the growing season showed a trend of first increasing and then decreasing with seasonal changes. The soil temperature gradually decreased from the surface to the deep layer, with daily average soil temperatures at points A, C, and D of 20.41, 18.95, and 22.1 $^{\circ}\text{C}$, respectively.

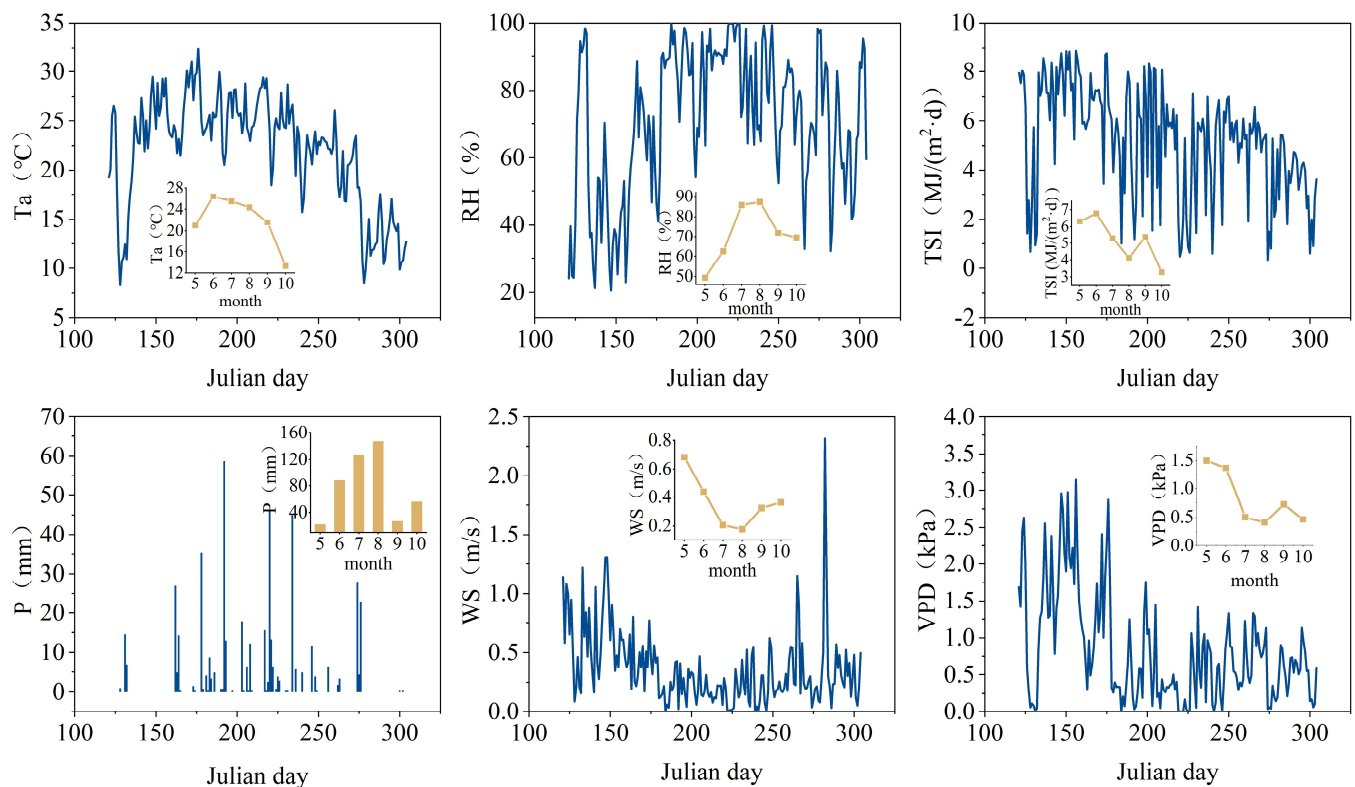


Figure 3. Diurnal changes of meteorological factors during the growing season in the study area in 2022. Abbreviations: Ta, temperature; TSI, total solar irradiance; RH, relative humidity; VPD, vapour pressure deficit; WS, wind speed; P, precipitation.

3.2. Characteristics of V Variation at Different Time Scales

Typical sunny, cloudy, and rainy days were selected to analyse the changes in V for different tree species in typical weather conditions (Figure 5). From the shape of V , all tree species showed a “single peak” curve on sunny days and a “double peak” curve on cloudy and rainy days, due to the influence of meteorological factors. V of each tree species began to increase at approximately 07:00 on sunny days and, after approximately 20:00, V gradually approached 0. Different tree species had different peak times and were maintained at high rates. The V values of H, SZ, YS, and CH were narrow, indicating that V maintained a high value for a short time, whereas the other tree species had a wide shape. The change times of cloudy and rainy days also changed compared to sunny days, with the start time being in the order sunny > cloudy > rainy and the stop time being rainy > cloudy > sunny. The variation in the amplitude of V made the difference in tree species on sunny days evident. The variation amplitudes of H, SZ, and YS were larger, indicating that the transpiration rate increased with increasing temperature on sunny days. The variation in the amplitude and mean value of V for each tree species decreased significantly on rainy and cloudy days. The change in the time of V for different months differed slightly (Figure 6). As the number of months increased, the start time was delayed, whereas the stop time gradually increased. The variation in V was larger in July and August and decreased significantly in October.

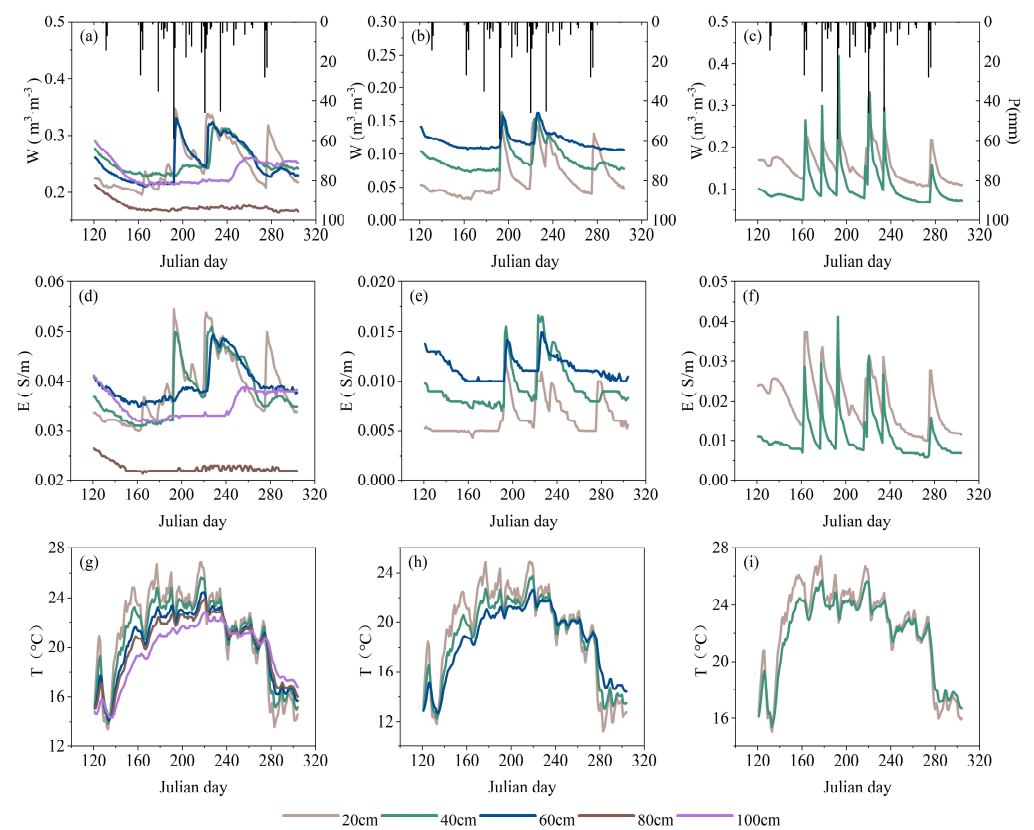


Figure 4. Daily changes of soil factors during the growth season in the study area in 2022. Subfigures (a–c) represent the daily variation of soil moisture content at sample points A, C, and D, respectively. Subfigures (d–f) represent the daily variation of soil conductivity at sample points A, C, and D, respectively. Subfigures (g–h) represent the daily variation of soil temperature at sample points A, C, and D, respectively. 20–100cm represents the depth of the soil layer. Abbreviations: W, soil moisture content; E, soil conductivity; T, soil temperature.

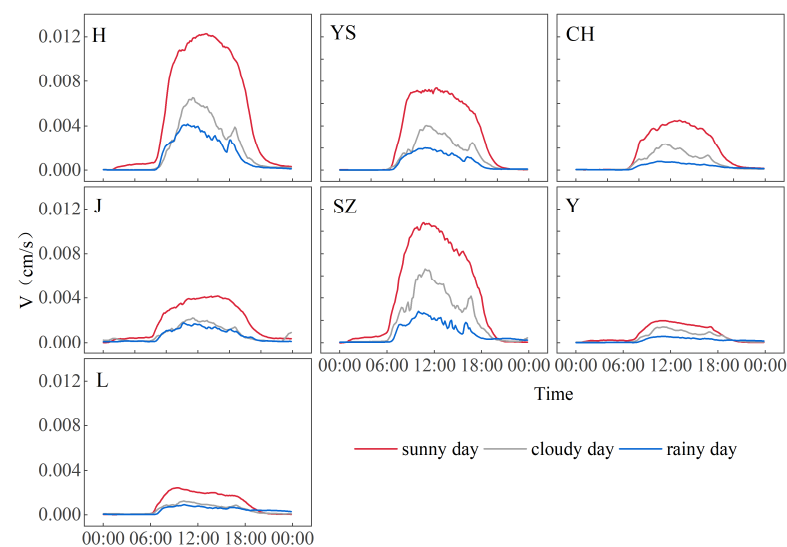


Figure 5. Characteristics of V changes in different tree species in typical weather conditions. H represents *Juglans regia*, YS represents *Populus hopeiensis*, CH represents *Robinia pseudoacacia*, SZ represents *Ziziphus jujuba* Mill. Var. *spinosa* (Bunge) Hu ex H. F. Chow., J represents *Vitex negundo* L. var. *heterophylla* (Franch.) Rehd., L represents *Koelreuteria paniculata* Laxm., Y represents *Pinus tabuliformis* Carr.

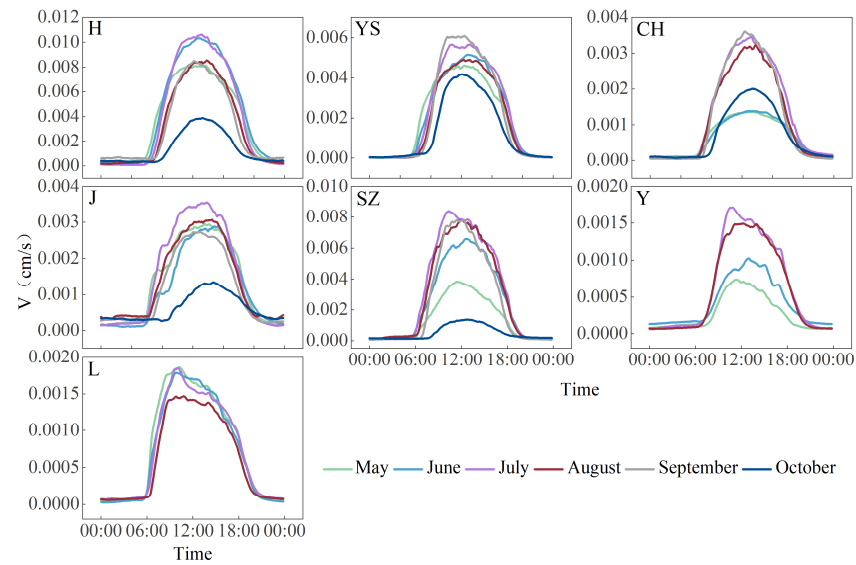


Figure 6. Variation characteristics of V in different tree species in different months. H represents *Juglans regia*, YS represents *Populus hopeiensis*, CH represents *Robinia pseudoacacia*, SZ represents *Ziziphus jujuba* Mill. Var. *spinosa* (Bunge) Hu ex H. F. Chow., J represents *Vitex negundo* L. var. *heterophylla* (Franch.) Rehd., L represents *Koelreuteria paniculata* Laxm., Y represents *Pinus tabuliformis* Carr.

The daily sap flow rates of the different tree species first increased and then decreased during the growing season. The fluctuations were small during the dry season and sharply fluctuated during the rainy season, due to the influence of meteorological factors (Figure 7). By month (Figure 8), V in May–June and September–October was relatively concentrated; in July–August it was more discrete, owing to fluctuations in environmental factors.

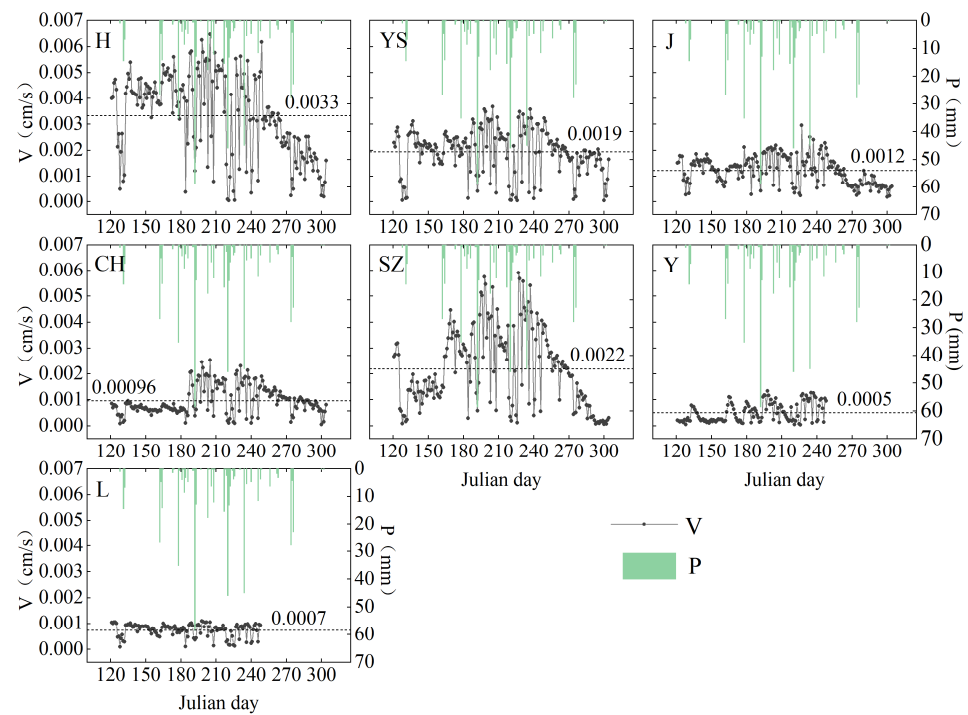


Figure 7. Dynamic changes of V of different tree species during the growing season. The dashed line represents the mean value of V in the growing season. H represents *Juglans regia*, YS represents *Populus hopeiensis*, CH represents *Robinia pseudoacacia*, SZ represents *Ziziphus jujuba* Mill. Var. *spinosa* (Bunge) Hu ex H. F. Chow., J represents *Vitex negundo* L. var. *heterophylla* (Franch.) Rehd., L represents *Koelreuteria paniculata* Laxm., Y represents *Pinus tabuliformis* Carr. P represents precipitation.

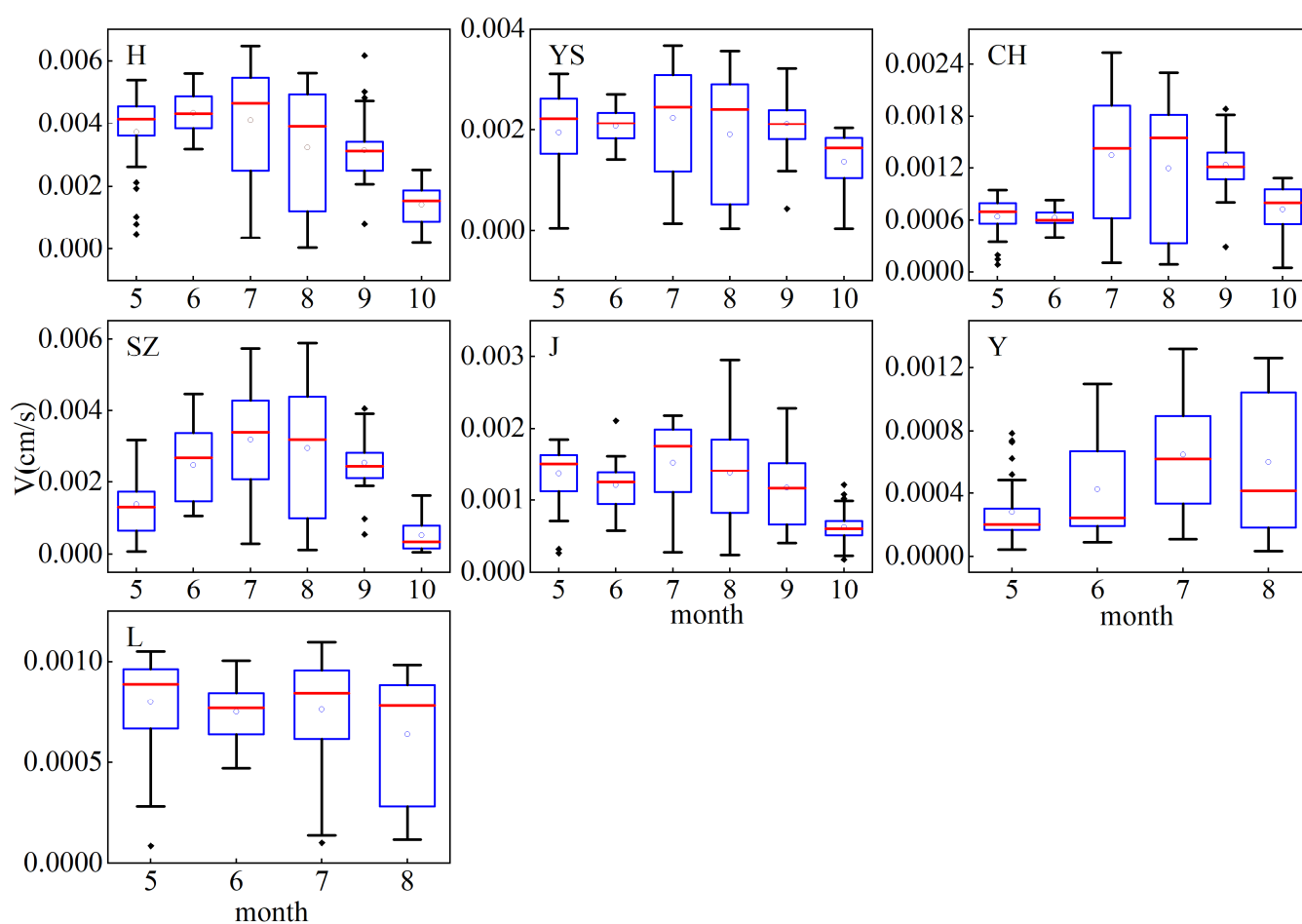


Figure 8. Dispersion degree of daily sap flow rate of different tree species in different months. The red lines in the box plot represent the median of V , and the hollow circles represent the average value of V . H represents *Juglans regia*, YS represents *Populus hopeiensis*, CH represents *Robinia pseudoacacia*, SZ represents *Ziziphus jujuba* Mill. Var. *spinosa* (Bunge) Hu ex H. F. Chow., J represents *Vitex negundo* L. var. *heterophylla* (Franch.) Rehd., L represents *Koelreuteria paniculata* Laxm., Y represents *Pinus tabuliformis* Carr.

3.3. Relationship between V and Environmental Factors

3.3.1. Pearson Correlation Analysis at Different Time Scales

The relationships between the V of different tree species and environmental factors at the hourly and daily scales were analysed by using the Pearson correlation analysis method, as shown in Figure 9. At the hourly scale, the correlation between V and the meteorological factors for various tree species was consistent. Except for RH and P, all meteorological factors showed significant positive correlations with V ($p < 0.01$), in a descending order of TSI (0.63–0.9, mean 0.81), Ta (0.37–0.63, mean 0.53), VPD (0.21–0.6, mean 0.46), RH (−0.47–−0.17, mean −0.35), WS (0.14–0.41, mean 0.32), and P (−0.09–−0.03, mean −0.07). The correlation between soil factors and V was weaker than that between meteorological factors. Except for W and E of H, which were negatively correlated with V , the soil factors of the other tree species were positively correlated with V . Overall, the correlation between T and V was strongest, followed by W and E.

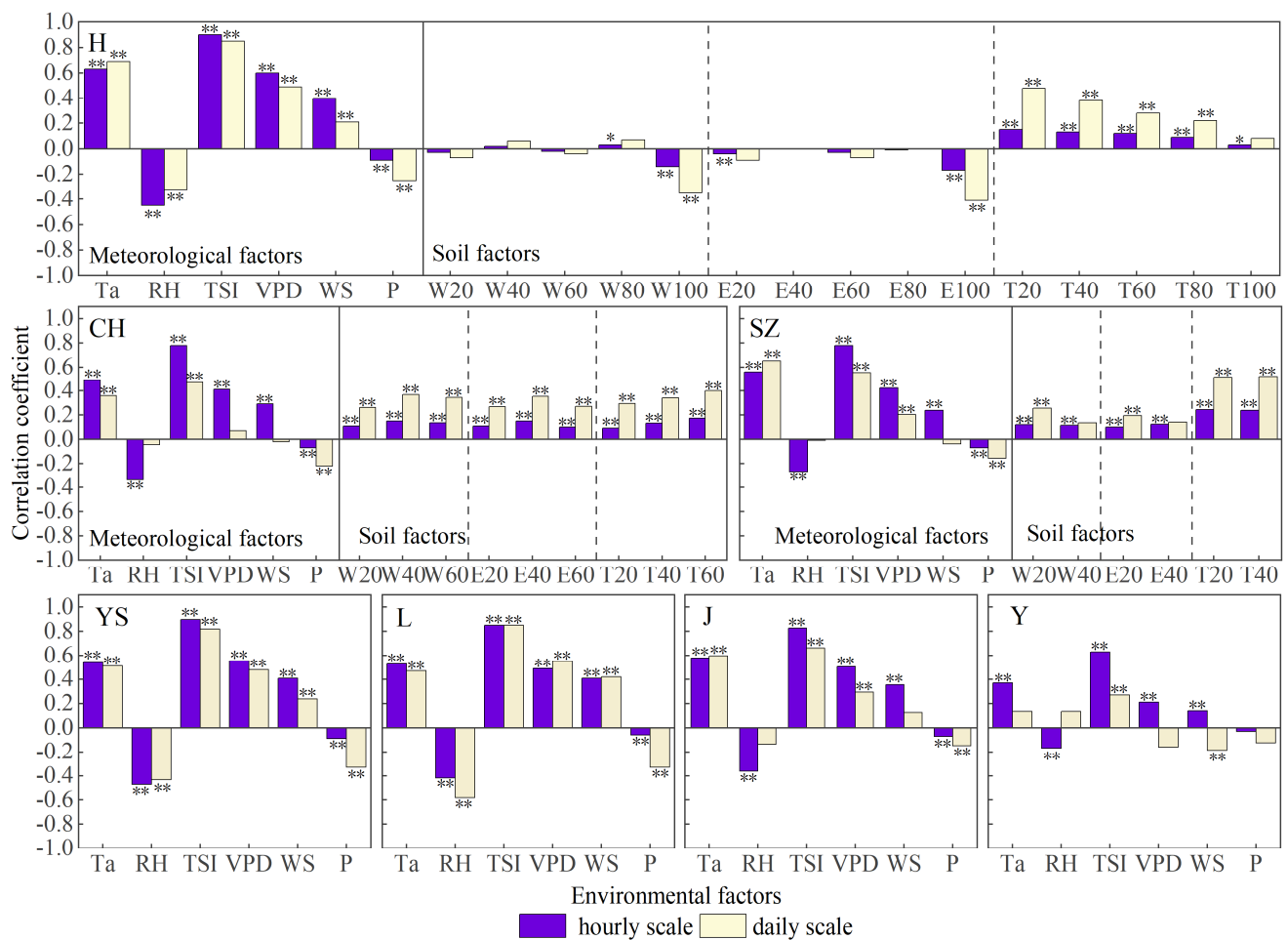


Figure 9. The correlation between V and environmental factors of various tree species at different time scales. * Represents a significant p -value at the 0.05 level, and ** represents a significant p -value at the 0.01 level. The dashed lines represent the segmentation line for different soil factors. W20–W100, E20–E100, T20–T100 represent the soil moisture content, soil conductivity, and soil temperature of the 20–100 cm soil layer, respectively. H represents *Juglans regia*, YS represents *Populus hopeiensis*, CH represents *Robinia pseudoacacia*, SZ represents *Ziziphus jujuba* Mill. Var. *spinosa* (Bunge) Hu ex H. F. Chow., J represents *Vitex negundo* L. var. *heterophylla* (Franch.) Rehd., L represents *Koelreuteria paniculata* Laxm., Y represents *Pinus tabuliformis* Carr. Abbreviations: Ta, temperature; TSI, total solar irradiance; RH, relative humidity; VPD, vapour pressure deficit; WS, wind speed; P, precipitation.

At the daily scale, except for P and Ta, the correlations between meteorological factors and V were weaker than those at the hourly scale. TSI was the most correlated factor with V (correlation coefficient 0.26–0.85) but the correlations between other meteorological factors and V led to differences between tree species: (1) except for the negative correlation between P, RH, and V of various tree species, the correlation between WS and V in CH, SZ, and Y shifted from a positive correlation on an hourly scale to a negative correlation on a daily scale. (2) The ranking of the correlation coefficients varied significantly among the tree species. For example, the order of H and YS correlation was TSI (0.85), Ta (0.69), VPD (0.49), RH (0.32), P (0.25), and WS (0.21), while the correlation coefficients of L were in the descending order of TSI (0.81), RH (0.55), VPD (0.53), Ta (0.47), WS (0.39), and P (0.31). In addition, the correlation between soil factors and V at the daily scale increased for all tree species, compared to that at the hourly scale. The correlation coefficients of some soil factors also exceeded those of some meteorological factors. On a daily scale, the correlation coefficients of all soil factors of the CH were greater than those of P, VPD, RH, and WS.

Through the above analysis of the correlation between V and environmental factors at different scales, we found that, regardless of the time scale, TSI, Ta, and V were highly correlated, whereas the correlation between other environmental factors and V was significantly different at different time scales and for different tree species. Among the soil factors, the correlation between T and V was stronger than that between the other two factors. In addition, the correlation between soil factors and V was more stable than that between meteorological factors and V, and changed synchronously with the time scale. Finally, with the increase in time scale (from hourly to daily), the correlation between most soil factors and V gradually increased, while the correlation between meteorological factors and V gradually decreased.

3.3.2. Impact of Environmental Factors on V at Different Time Scales

The relative importance of environmental factors to V was evaluated based on random forest and stepwise regression R^2 variations, before the differences between the two methods were analysed.

The random forest results showed that (Figure A1) at the hourly scale, TSI was the most important environmental factor affecting the V of various tree species, with an importance ratio ranging from 81.8% to 96.4%, in contrast to the ratios of other environmental factors, which were relatively small. At the daily scale, except for CH and SZ, TSI was still the most important influencing factor in other tree species, but its importance was weaker compared with that at the hourly scale, accounting for 30.3–73.6%, while the importance of other environmental factors to V gradually increased. The meteorological factors VPD, RH, and Ta had significant impacts on V. In addition, the importance of soil factors increased with time; soil conductivity and temperature in the shallow layer (20–40 cm) were the main factors affecting V in H, CH, and SZ. Stepwise linear regression (Tables 2 and 3) revealed that TSI had the greatest influence on V at both the hourly and daily scales, with its R^2 variation ranging from 0.41–0.82. In addition, with the increase in the time scale, the degree of influence of TSI decreased, with the change in R^2 being between 0.067–0.722. In addition, the number of environmental factors affecting vegetation transpiration rate decreased.

Table 2. Stepwise linear regression R^2 variation between V and environmental factors in YS, J, Y, L. YS represents *Populus hopeiensis*, J represents *Vitex negundo* L. var. *heterophylla* (Franch.) Rehd., L represents *Koelreuteria paniculata* Laxm., Y represents *Pinus tabulaformis* Carr. Abbreviations: Ta, temperature; TSI, total solar irradiance; RH, relative humidity, VPD, vapour pressure deficit; WS, wind speed; P, precipitation.

	YS		J		Y		L	
	Hourly Scale	Daily Scale	Hourly Scale	Daily Scale	Hourly Scale	Daily Scale	Hourly Scale	Daily Scale
TSI	0.805	0.669	0.686	0.436	0.408	0.067	0.735	0.723
Ta	0.004	- ¹	0.023	0.033	0.012	0.23	0.001	-
VPD	0.001	-	0.008	-	0.05	-	0.002	-
RH	0.017	-	0.001	0.126	0.032	-	0.015	-
WS	0.002	0.017	0.000	-	0.011	-	-	-
P	-	-	-	-	0.001	-	-	-

¹—indicated that the environmental factor had not entered the stepwise regression equation.

Combining the analysis results of the above two methods showed that the dominant factor affecting V at the hourly and daily scales was TSI. The interpretive rates of TSI were 92.5% (random forest) and 67.7% (stepwise linear regression) on an hourly scale, and 41.5% (random forest) and 46.5% (stepwise linear regression) on a daily scale. In general, the degree of importance of meteorological factors was greater than that of the soil factors. In addition, both methods showed that the importance of the TSI diminished and the importance of other factors increased, when moving from the hourly to the daily scale.

Table 3. Stepwise linear regression R^2 variation between V and environmental factors in H, CH, SZ. W20–W100, E20–E100, T20–T00 represent the soil moisture content, soil conductivity, and soil temperature of the 20–100 cm soil layer, respectively. H represents *Juglans regia*, CH represents *Robinia pseudoacacia*, SZ represents *Ziziphus jujuba* Mill. Var. *spinosa* (Bunge) Hu ex H. F. Chow. Abbreviations: Ta, temperature; TSI, total solar irradiance; RH, relative humidity, VPD, vapour pressure deficit; WS, wind speed; P, precipitation.

	H		CH		SZ	
	Hourly Scale	Daily Scale	Hourly Scale	Daily Scale	Hourly Scale	Daily Scale
TSI	0.812	0.722	0.604	0.218	0.686	0.422
Ta	0.027	0.081	0.015	0.059	0.023	0.059
VPD	0.002	- ¹	0.009	0.001	0.013	0.100
RH	0.000	0.034	0.002	0.014	0.001	-
WS	0.001	-	0.020	-	0.001	-
P	0.001	-	-	-	0.001	-
W20	0.002	0.005	-	-	0.009	0.010
W40	-	-	0.005	-	-	0.082
W60	-	-	-	-	-	-
W80	0.001	-	-	-	-	-
W100	0.001	-	-	-	-	-
EC20	-	-	-	-	-	0.056
EC40	-	-	-	-	-	-
EC60	-	-	0.018	0.090	-	-
EC80	-	0.007	-	-	-	-
EC100	-	-	-	-	-	-
T20	0.001	-	0.001	-	0.006	0.009
T40	0.001	-	0.016	0.084	0.002	0.082
T60	-	-	0.036	0.187	-	-
T80	-	-	-	-	-	-
T100	-	-	-	-	-	-

¹—indicated that the environmental factor had not entered the stepwise regression equation.

3.3.3. Time Lag Effect of the Sap Flow

When analysing the relationship between V and the driving factor at the hourly scale, we found that there was a “hysteresis loop” phenomenon between V and meteorological factors. Taking TSI and VPD as examples, the time-lag effect was manifested by the mismatch of the fitting curves of the correlation between the morning and afternoon periods. With the gradual enhancement of the driving factors, V continued to increase until saturation. When the influence of the driving factor was weakened, the V decay ratio differed from that of the increase, resulting in a receding path that did not coincide with the increasing path. Therefore, in this study, the relationship between V and driving factors can be categorised according to the relative magnitude of the increase and decay ratio: (1) clockwise time-delay loop: under the same value of a certain driving factor, V in the morning is higher than that in the afternoon; (2) counterclockwise time-delay loop: under the same value of a driving factor, the V in the afternoon is higher than that in the morning; (3) “8” time-lag loop: before a certain moment, the V in the morning is higher (lower) than that in the afternoon under the same driving factor; after this moment, the V in the morning is lower (higher) than that in the afternoon. We found that the V and VPD of all tree species formed a clockwise hysteretic loop, whereas the time-lag response loop with TSI was relatively complex among different tree species. Specifically, H, CH, and J were counter-clockwise time-lag loops; SZ and L were clockwise time-delay loops; and YS and Y were “8” time-delay loops (Figure 10).

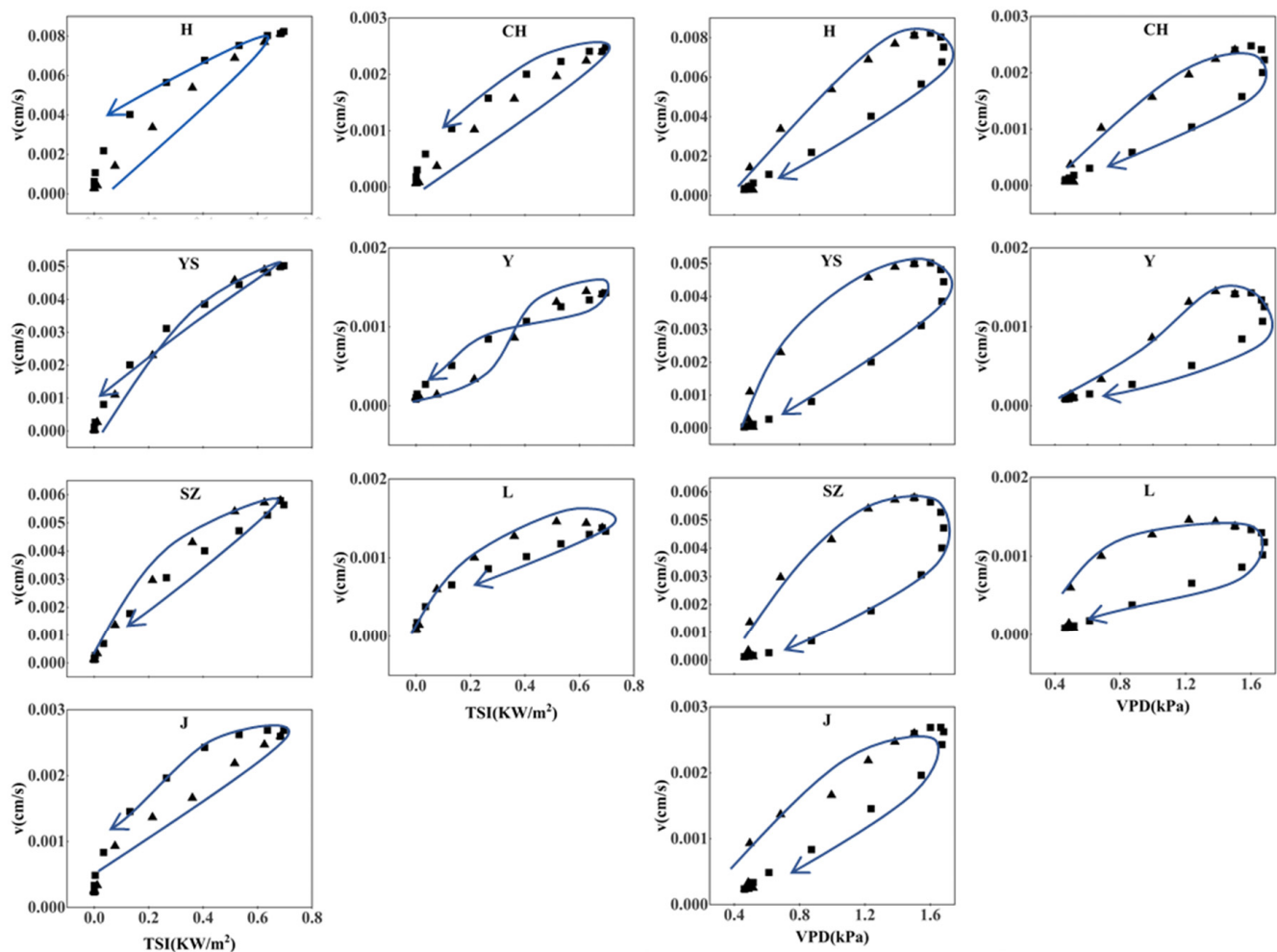


Figure 10. V Fitting results with TSI and VPD. Triangle point data represents the morning period, while square point data represents the afternoon period. The blue arrows represent the type of time–lag loop for V. H represents *Juglans regia*, YS represents *Populus hopeiensis*, CH represents *Robinia pseudoacacia*, SZ represents *Ziziphus jujuba* Mill. Var. *spinosa* (Bunge) Hu ex H. F. Chow., J represents *Vitex negundo* L. var. *heterophylla* (Franch.) Rehd., L represents *Koelreuteria paniculata* Laxm., Y represents *Pinus tabuliformis* Carr. Abbreviations: TSI, total solar irradiance; VPD, vapour pressure deficit.

To further determine the delay response time of V and each driving factor, a dislocation analysis method was used to analyse the delay length of V and each meteorological factor. The lag response time was determined by analysing the correlation between the hourly scale sap flow rate data and the driving factor in the 1-h step. The results showed that, except for L, the other tree species showed no lag effect between V and TSI, with an average correlation coefficient of 0.93 and 0.99 (Figure A2). VPD, RH, and T_a lagged V for 1–2 h, with average correlation coefficients of 0.93–0.99, -0.99 – -0.96 , and 0.97–0.99, respectively. WS lagged V by 1 h did not have a time lag effect, and had an average correlation coefficient of 0.86–0.93.

3.3.4. Response Models of V and Environmental Factors at Different Time Scales

A stepwise regression method was used to construct a response model for the hourly and daily V and environmental factors. Additionally, two schemes were considered in the hourly regression model. One scheme was to construct a regression model by using the original data without considering the time-lag effect of V and meteorological factors, and the other was to construct the model considering the time-lag effect of V. Then, the fitting

effects of the two schemes were compared. According to the constructed model and fitting results (Table A1), we found that: (1) according to the accuracy of the model, all tree species except Y had better fitting at all time scales and a fitting degree above 0.59. When the timescale of most species increased from the hourly to the daily scale, the degree of fitting gradually decreased. (2) The V of each tree species at an hourly scale was comprehensively affected by multiple environmental factors. As the timescale increased, the number of factors that needed to be considered in the response model decreased. (3) The accuracy of the regression model of V and the environmental factors constructed by considering the time lag effects both improved, and the fitting accuracy of L and Y significantly improved (Figure A3).

4. Discussion

4.1. V Responds to Environmental Factors

The change in V is affected by the surrounding environmental factors. In this study, the correlation between the V of each tree species and meteorological factors was mainly negatively correlated with RH and P, and was mainly positively correlated with other meteorological factors ($p < 0.01$). TSI, VPD, and Ta had the strongest correlations with V, which is consistent with the results of previous studies [20,55–58]. TSI is the main source of energy for photosynthesis in plants and affects transpiration by inducing stomatal opening for water vapour exchange [3,59,60]. VPD affects the transpiration rate of vegetation by altering the stomatal conductance and air resistance [43,61,62]. However, some studies determined that when VPD is greater than a certain value, it also has a certain inhibitory effect on V. For example, Meinzer et al. (1993) found that in the humid forests of central and northern South America, stomata gradually close with increasing VPD when VPD exceeds 1.5 kPa. Pataki et al. (2000) and Ewers et al. (2002) found a nonlinear relationship between V and VPD, where V initially increased and then often decreased, owing to stomatal closure when VPD was high.

In addition, while many studies have demonstrated the importance of soil water stress on V [25,39,63–66], the influence of other soil factors (such as soil temperature) on V cannot be ignored. The present study found that soil temperature had a greater impact on V than the other two factors, which was consistent with the results of Sun et al. (2022). Changes in soil temperature significantly influenced the water absorption capacity of plant roots. When the soil temperature is too low, the respiration rate of roots decreases and the active water absorption weakens. However, low temperatures affect the permeability of root cell membranes, which is associated with changes in aquaporin activity, thus affecting root water absorption [67–69]. However, when the soil temperature is too high, the lignification degree of roots increases and the ageing process of roots is accelerated, thus reducing the water absorption and transport capacity of roots, resulting in stomatal opening and a reduced transpiration rate [70]. We also found that soil water and electrical conductivity at 100 cm of H had a greater influence on V, whereas soil water and electrical conductivity at 20–40 cm of CH and SZ had a greater influence on V, indicating that a large number of fine plant roots may be distributed in this range and that the change in water content in the shallow layer affected the water absorption capacity of plant roots.

The study also found that the relationship between the V of different tree species and environmental factors differed with the timescale. With an increase in the time scale, the correlation between subsurface factors and V was gradually enhanced, whereas the effect of meteorological factors gradually weakened. This may be because, at a small scale, the change in V is more sensitive to fluctuations in meteorological factors (such as Ta, TSI, and VPD) and the two show relatively synchronous change characteristics. On a daily scale, the sensitivity of V to soil factors was enhanced due to the time–accumulation effect.

4.2. Time-Lag Effect of Sap Flow on Environmental Factors

Our research showed that incorporating time–lag effects into the regression model of V and environmental factors can improve the fitting accuracy of the model, indicating that

it is an important variable in sap flow modelling. In this study, there was a 1-h lag between V and RH, V and Ta, and V and VPD of various tree species during the growing season. However, except for L, no significant time-lag effect was observed for sap flow or TSI in the other tree species, which was consistent with the results of previous studies [44,61,71]. The time-lag effect is the result of the stomatal response to internal and external factors in trees, with TSI and VPD playing more important roles than other environmental factors. It has been reported that soil water content and potential determine the amount of water supplied by transpiration and thus regulate the lag time of sap flow and meteorological factors [1,72,73]. In the environmental conditions of soil drought or high evaporation demand, plants regulate transpiration earlier by reducing stomatal conductance and the time lag between sap flow and VPD is longer [74,75]. For example, when the soil moisture was sufficient, the sap flow peak of *Fagus longipetiolata* occurred 20–40 min earlier than the peak of VPD, and 40–60 min earlier than the peak of soil moisture deficiency [31]. In relatively dry conditions, the time lag between the peak sap flow and the peak VPD of *Chamaecyparis obtusa* was approximately 60–180 min, and was less than 60 min in relatively humid soil conditions [76].

Plant properties regulate access to water and light, thus controlling the occurrence of time-lag phenomena. For example, Wan, et al. [77] found that the sapwood of plants has a certain controlling effect on the delay in sap flow, which may be related to stem water storage. The measured V exhibited a slower response to solar radiation in trees with larger sapwood and higher water storage capacity. In addition, O'Brien, et al. [78] found that tree height significantly affects sap flow, with taller trees responding more quickly to changes in environmental variables than shorter trees. High vine coverage buffered the response of tree sap flow to weather. In addition, tree DBH [79], canopy development [41], and tree age [76] also affect the time lag of sap flow and its driving factors.

In addition, the time-lag effect of sap flow varies significantly by season [44]. In this study, using VPD and TSI as examples, we found significant differences in the lag length between V and meteorological factors among different tree species in different months (Figure A4). For example, we did not find a time-lag effect between the V and TSI of different tree species in the growing season and instead found more details in different months. It is worth noting that V did not lag or lead the driving factor of each tree species and showed a certain regularity with the increase of months. In general, the time-lag effect should be considered in sap flow prediction, particularly in different months, as otherwise there may be some errors [75].

4.3. Limitations

On the basis of measured sap flow data, this study investigated sap flow rate changes and responses to environmental factors in seven typical tree species in the hilly areas of the Haihe River basin during the growing season of 2022. Although important fundamental results were achieved, this study had some limitations.

- (1) The time-lag effect of plant sap flow was confirmed in relation to meteorological factors, such as VPD and TSI, but its mechanism is still unclear. As discussed in Section 4.2, the time-lag effect of plant sap flow is the result of a combination of factors, such as weather, soil, and tree growth conditions. Future studies should address changes in these factors, with the aim of revealing specific response rules. In addition, we should strengthen the study of the synergistic effect of environmental factors on time-lag effect, so as to understand the sap flow characteristics from the perspective of time-lag characteristics.
- (2) Given the constraints of experimental conditions, the sample size of this study was relatively modest and its temporal and spatial scales were restricted. Consequently, the results only depicted the response rule within the specific environmental conditions of the study area, and may not be generalizable to other watersheds. Thus, it may be beneficial in future to augment the number of samples and conduct sap flow monitoring trials across varying climatic conditions. This could enhance our

understanding of tree species' transpiration and water use, and assist the examination of the effect of environmental factors on these processes.

- (3) Our study focused solely on variations in sap flow rates across varietal trees, neglecting the overall tree transpiration. Nonetheless, understanding the significance of tree transpiration is essential for comprehending local ecosystem water consumption and effective water resource stewardship. Future research should intensely examine changes in tree transpiration and their correlation with environmental conditions.

5. Conclusions

This study used sap flow data from the 2022 growing season to analyse the change characteristics of the sap flow rate of seven typical tree species in the hilly areas of the Haihe River Basin in China at different time scales. The relationship between sap flow and environmental factors at different time scales was quantitatively analysed and a response model was constructed. The time–delay effect of sap flow and environmental factors were included in the model to analyse the simulation effect. By analysing the correlation between sap flow and environmental factors, it was found that TSI was the most important environmental factor affecting sap flow at the hourly and daily scales. With an increase in the time scale, the correlation between meteorological factors and sap flow rate gradually weakened, whereas the correlation between most soil factors and sap flow rate gradually increased. The established response model showed that the fit of all tree species, except Y, was better at all timescales, with a fitting degree above 0.59. When the timescale of most tree species increased from the hour to the day scale, the degree of fit gradually weakened. The accuracy of the regression model based on the time–lag effect improved and the accuracy of the fitting of L and Y also improved significantly.

Author Contributions: Conceptualization, Y.Z. and S.H.; methodology, Q.W. and S.H.; software, S.H. and Y.H.; validation, S.H. and X.W.; formal analysis, S.H.; investigation, S.H., X.L. and L.L.; resources, S.H.; data curation, S.H.; writing—original draft preparation, S.H.; writing—review and editing, Y.Z. and J.C.; visualization, S.H.; supervision, Q.W., J.Z. and H.L.; project administration, Q.W.; funding acquisition, Y.Z. and J.Z. All authors have read and agreed to the published version of the manuscript.

Funding: The research was funded by the National Key Research and Development Program of China (2021YFC3200205), the National Science Fund for Distinguished Young Scholars of China (52025093), the Free Exploration Project of State Key Laboratory of Simulation and Regulation of Water Cycle in River Basin (SKL2022TS01), the Significant Science and Technology Project of the Ministry of Water Resources (SKR-2022056) and the National Natural Sciences Foundation of China (42371048).

Data Availability Statement: The data that support the study findings are available from the corresponding author upon reasonable request.

Acknowledgments: We are very grateful to the editor for their comments and suggestions, which have substantially contributed to the improvement of the paper.

Conflicts of Interest: The authors declare no conflicts of interest.

Appendix A

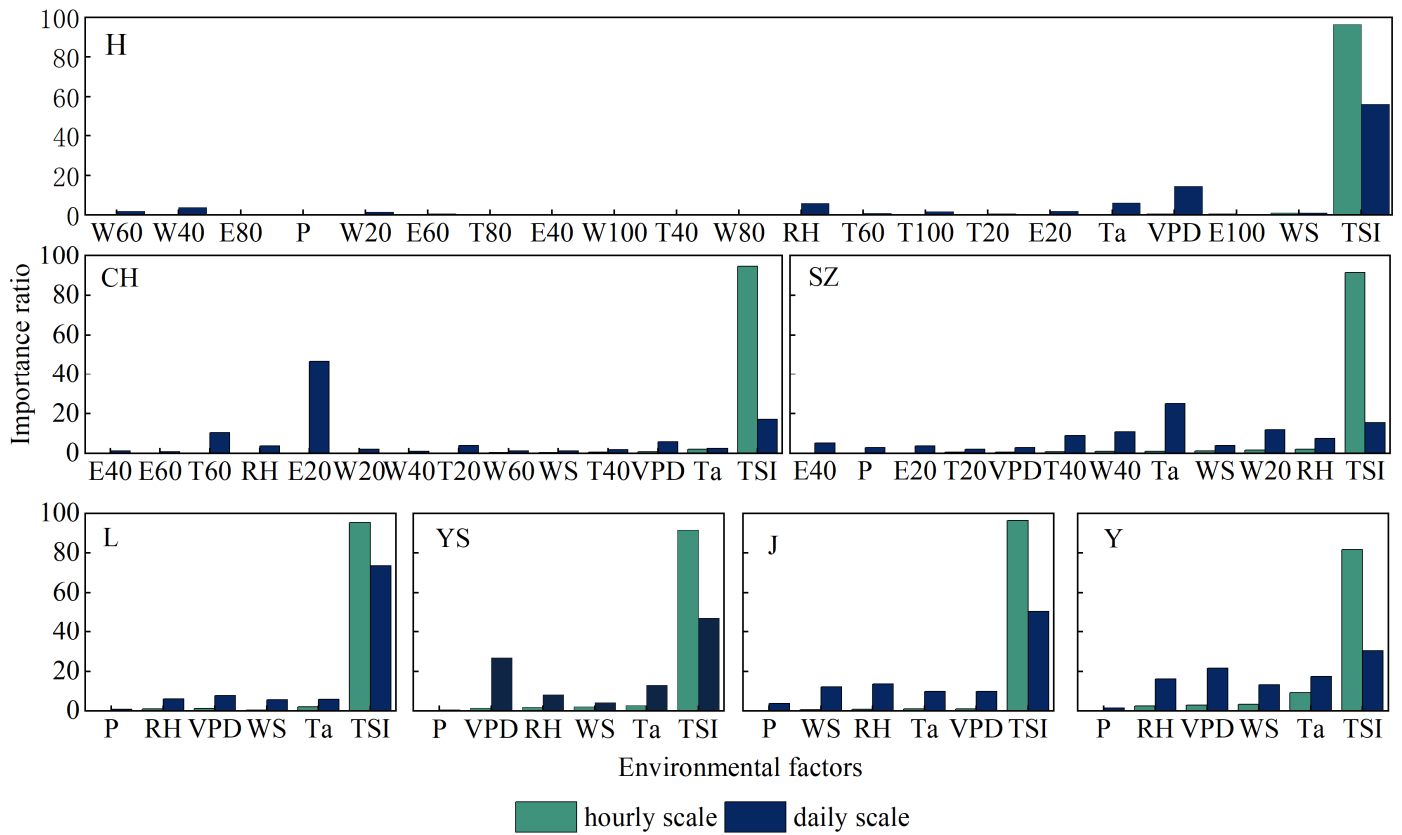


Figure A1. Ranking the importance of environmental factors to V based on the random forest method. W20–W100, E20–E100, T20–T00 represent the soil moisture content, soil conductivity, and soil temperature of the 20–100cm soil layer, respectively. H represents *Juglans regia*, YS represents *Populus hopeiensis*, CH represents *Robinia pseudoacacia*, SZ represents *Ziziphus jujuba* Mill. Var. *spinosa* (Bunge) Hu ex H. F. Chow., J represents *Vitex negundo* L. var. *heterophylla* (Franch.) Rehd., L represents *Koelreuteria paniculata* Laxm., Y represents *Pinus tabuliformis* Carr. Abbreviations: Ta, temperature; TSI, total solar irradiance; RH, relative humidity; VPD, vapour pressure deficit; WS, wind speed; P, precipitation.

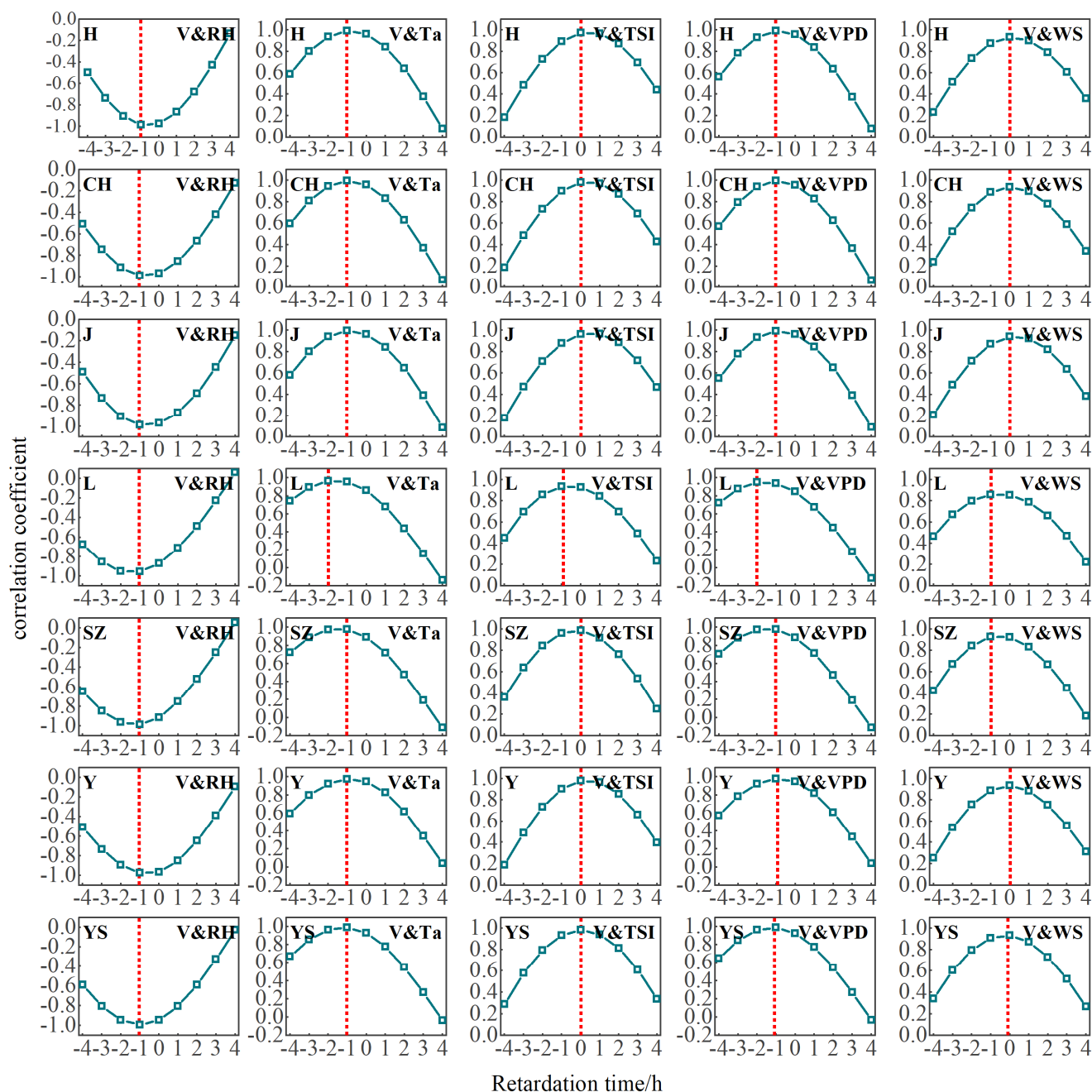


Figure A2. Time–lag length between V and various meteorological factors. The red dashed lines represent the retardation time corresponding to the maximum correlation coefficient between V and environmental factors. In the horizontal coordinate, $-4\sim-1$ indicates that V is 1–4 h ahead of the meteorological factor, and $1\sim4$ indicates that V is 1–4 h behind the meteorological factor. H represents *Juglans regia*, YS represents *Populus hopeiensis*, CH represents *Robinia pseudoacacia*, SZ represents *Ziziphus jujuba* Mill. Var. *spinosa* (Bunge) Hu ex H. F. Chow., J represents *Vitex negundo* L. var. *heterophylla* (Franch.) Rehd., L represents *Koelreuteria paniculata* Laxm., Y represents *Pinus tabuliformis* Carr. Abbreviations: Ta, temperature; TSI, total solar irradiance; RH, relative humidity; VPD, vapour pressure deficit; WS, wind speed; P, precipitation.

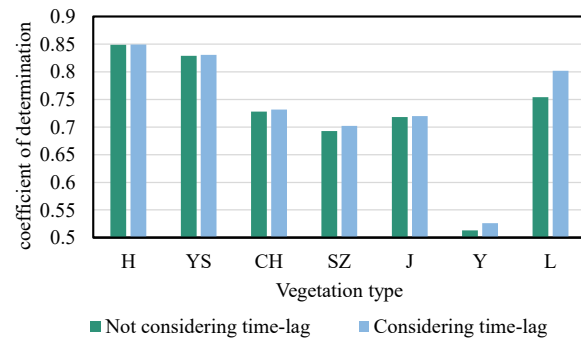


Figure A3. Comparison of fitting accuracy between response models, with and without time-lag effects. H represents *Juglans regia*, YS represents *Populus hopeiensis*, CH represents *Robinia pseudoacacia*, SZ represents *Ziziphus jujuba* Mill. Var. *spinosa* (Bunge) Hu ex H. F. Chow., J represents *Vitex negundo* L. var. *heterophylla* (Franch.) Rehd., L represents *Koelreuteria paniculata* Laxm., Y represents *Pinus tabuliformis* Carr.

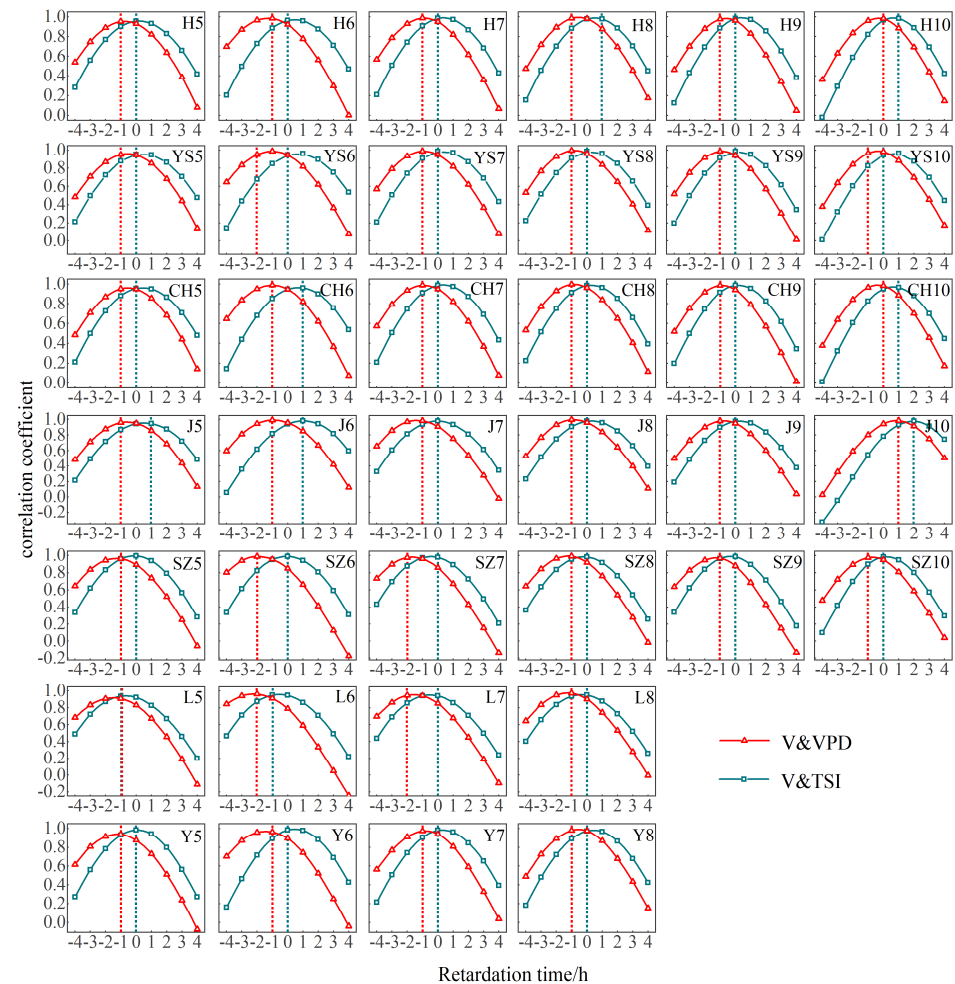


Figure A4. Time-lag length between V and TSI, VPD in different months. The red and green dashed lines represent the retardation time corresponding to the maximum correlation coefficient between V and TSI, VPD, respectively. H represents *Juglans regia*, YS represents *Populus hopeiensis*, CH represents *Robinia pseudoacacia*, SZ represents *Ziziphus jujuba* Mill. Var. *spinosa* (Bunge) Hu ex H. F. Chow., J represents *Vitex negundo* L. var. *heterophylla* (Franch.) Rehd., L represents *Koelreuteria paniculata* Laxm., Y represents *Pinus tabuliformis* Carr. Abbreviations: TSI, total solar irradiance; VPD, vapour pressure deficit.

Table A1. Response model of V and environmental factors. W20–W100, E20–E100, T20–T00 represent the soil moisture content, soil conductivity, and soil temperature of the 20–100 cm soil layer, respectively. H represents *Juglans regia*, YS represents *Populus hopeiensis*, CH represents *Robinia pseudoacacia*, SZ represents *Ziziphus jujuba* Mill. Var. *spinosa* (Bunge) Hu ex H. F. Chow., J represents *Vitex negundo* L. var. *heterophylla* (Franch.) Rehd., L represents *Koelreuteria paniculata* Laxm., Y represents *Pinus tabuliformis* Carr. Abbreviations: Ta, temperature; TSI, total solar irradiance; RH, relative humidity, VPD, vapour pressure deficit; WS, wind speed; P, precipitation.

Tree Name	Time Scale	Response Model	Fitting Degree
H	hourly	$V = -0.00218 + 0.00994TSI + 0.00021Ta + 0.00197SW20 + 0.03345SW80 - 0.00039WS - 0.00037T20 - 0.01503SW100 + 0.00029T40 - 0.00011P - 0.00002RH - 0.00056VPD$	0.849
	hourly (considered time-lag)	$V = -0.0016 + 0.01TSI + 0.00019Ta + 0.0031SW20 + 0.022SW80 - 0.00034WS - 0.0094SW100 + 0.0012T80 - 0.000024RH - 0.00066VPD - 0.000092P - 0.00063T100 - 0.00058T40$	0.849
	daily	$V = -0.00745 + 0.00063TSI + 0.00008Ta + 0.00002RH + 0.16059EC80 + 0.00333SW20$	0.849
YS	hourly	$V = 0.002 + 0.007TSI + 0.000076Ta - 0.001VPD - 0.000036RH - 0.00027WS$	0.829
	hourly (considered time-lag)	$V = 0.0022 + 0.0071 TSI + 0.000081 Ta - 0.000036 RH - 0.00098 VPD - 0.0003 WS$	0.831
	daily	$V = 0.00030 + 0.00035TSI - 0.00042WS$	0.687
CH	hourly	$V = -0.00140 + 0.00279TSI + 0.00044T60 - 0.00027T40 + 0.00009Ta + 0.09925EC60 - 0.00059VPD - 0.00002RH - 0.00026WS - 0.11215EC40 + 0.01070SW40 - 0.00012T20$	0.728
	hourly (considered time-lag)	$V = -0.00153 + 0.00285 TSI + 0.00056 T60 - 0.00049 T40 + 0.00008 Ta + 0.10494 EC60 - 0.00002 RH - 0.00061 VPD - 0.00023 WS - 0.11425 EC40 + 0.01052 SW40$	0.732
	daily	$V = -0.00248 + 0.00015TSI + 0.00046T60 - 0.00040T40 + 0.11147EC60 + 0.00006Ta - 0.00036VPD - 0.00001RH$	0.667
SZ	hourly	$V = -0.0043 + 0.0075TSI + 0.00074T40 + -0.00078 + -0.00064T20 + 0.00013Ta + 0.022SW20 - 0.091EC20 - 0.02SW40 + 0.17EC40 - 0.00047VPD - 0.000014RH$	0.693
	hourly (considered time-lag)	$V = -0.00420 + 0.00639 TSI + 0.00093 T40 - 0.00086 T20 + 0.00019 Ta - 0.00073 WS + 0.01960 SW20 - 0.08073 EC20 - 0.02018 SW40 + 0.18234 EC40 - 0.00001 RH - 0.00032 VPD$	0.702
	daily	$V = -0.00545 + 0.00027Ta + 0.00034TSI - 0.00030VPD + 0.02192SW20 - 0.07099EC20 - 0.00126T200.00123T40 - 0.00658SW40$	0.751
J	hourly	$V = -0.00012 + 0.00336TSI + 0.00005Ta - 0.00026VPD - 0.000003RH - 0.00003P$	0.718
	hourly (considered time-lag)	$V = -0.0000015 + 0.0033573 TSI + 0.0000527 Ta - 0.0003161 VPD - 0.0000053 RH - 0.0000254 P$	0.720
	daily	$V = -0.00095 + 0.00019TSI + 0.00001RH + 0.00002Ta$	0.594
Y	hourly	$V = 0.001 + 0.002TSI - 0.001VPD + 0.000035Ta - 0.000016RH - 0.00021WS + 0.000027P$	0.513
	hourly (considered time-lag)	$V = 0.00127 + 0.00203 TSI - 0.00067 VPD - 0.00002 RH + 0.00003 Ta - 0.00020 WS + 0.00003 P$	0.526
	daily	$V = 0.00014 + 0.00011TSI - 0.00030VPD$	0.296

Table A1. Cont.

Tree Name	Time Scale	Response Model	Fitting Degree
L	hourly	$V = 0.00082 + 0.0022\text{TSI} + 0.000023\text{Ta} - 0.00033\text{VPD} - 0.00001\text{RH} + 0.00002\text{P}$	0.754
	hourly (considered time-lag)	$V = 0.00048 + 0.00207\text{TSI} + 0.00002\text{Ta} - 0.00001\text{RH} - 0.00017\text{VPD} + 0.00003\text{P} - 0.00006\text{WS}$	0.802
	daily	$V = 0.00023 + 0.000091\text{TSI}$	0.723

References

- Hong, L.; Guo, J.; Liu, Z.; Wang, Y.; Ma, J.; Wang, X.; Zhang, Z. Time-Lag Effect between Sap Flow and Environmental Factors of *Larix principis-rupprechtii* Mayr. *Forests* **2019**, *10*, 971. [\[CrossRef\]](#)
- Daley, M.J.; Phillips, N.G. Interspecific variation in nighttime transpiration and stomatal conductance in a mixed New England deciduous forest. *Tree Physiol.* **2006**, *26*, 411–419. [\[CrossRef\]](#)
- Liu, J.; Zhao, Y.; Wang, Y.; Zhang, J.; Xue, J.; Wang, S.; Chang, J. Sap flow of two typical woody halophyte species responding to the meteorological and irrigation water conditions in Taklimakan Desert. *Ecohydrol. Hydrobiol.* **2023**, *26*, 411–419. [\[CrossRef\]](#)
- Jasechko, S.; Sharp, Z.D.; Gibson, J.J.; Birks, S.J.; Yi, Y.; Fawcett, P.J. Terrestrial water fluxes dominated by transpiration. *Nature* **2013**, *496*, 347–350. [\[CrossRef\]](#) [\[PubMed\]](#)
- Small, E.E.; McConnell, J.R. Comparison of soil moisture and meteorological controls on pine and spruce transpiration. *Ecohydrology* **2008**, *1*, 205–214. [\[CrossRef\]](#)
- Song, L.N.; Zhu, J.J.; Zheng, X.; Wang, K.; Lü, L.Y.; Zhang, X.L.; Hao, G.Y. Transpiration and canopy conductance dynamics of *Pinus sylvestris* var. *mongolica* in its natural range and in an introduced region in the sandy plains of Northern China. *Agric. For. Meteorol.* **2020**, *281*, 14. [\[CrossRef\]](#)
- Aranda, I.; Forner, A.; Cuesta, B.; Valladares, F. Species-specific water use by forest tree species: From the tree to the stand. *Agric. Water Manag.* **2012**, *114*, 67–77. [\[CrossRef\]](#)
- Ford, C.R.; Hubbard, R.M.; Vose, J.M. Quantifying structural and physiological controls on variation in canopy transpiration among planted pine and hardwood species in the southern Appalachians. *Ecohydrology* **2011**, *4*, 183–195. [\[CrossRef\]](#)
- COHEN, Y.; GREEN, M.F.G.C. Improvement of the heat pulse method for determining sap flow in trees. *Plant Cell Environ.* **1981**, *4*, 391–397. [\[CrossRef\]](#)
- Chang, X.X.; Zhao, W.Z.; Zhang, Z.H.; Su, Y.Z. Sap flow and tree conductance of shelter-belt in and region of China. *Agric. For. Meteorol.* **2006**, *138*, 132–141. [\[CrossRef\]](#)
- Cienciala, E.; Lindroth, A.; Čermák, J.; Hällgren, J.-E.; Kučera, J. Assessment of transpiration estimates for *Picea abies* trees during a growing season. *Trees* **1992**, *6*, 121–127. [\[CrossRef\]](#)
- Poyatos, R.; Čermák, J.; Llorens, P. Variation in the radial patterns of sap flux density in pubescent oak (*Quercus pubescens*) and its implications for tree and stand transpiration measurements. *Tree Physiol.* **2007**, *27*, 537–548. [\[CrossRef\]](#)
- Granier, A. Evaluation of transpiration in a Douglas-fir stand by means of sap flow measurements. *Tree Physiol.* **1987**, *3*, 309–3320. [\[CrossRef\]](#) [\[PubMed\]](#)
- Nadezhdina, N.; Čermák, J.; Ceulemans, R. Radial patterns of sap flow in woody stems of dominant and understory species: Scaling errors associated with positioning of sensors. *Tree Physiol.* **2002**, *22*, 907–918. [\[CrossRef\]](#) [\[PubMed\]](#)
- Fiora, A.; Cescatti, A. Vertical foliage distribution determines the radial pattern of sap flux density in *Picea abies*. *Tree Physiol.* **2008**, *28*, 1317–1323. [\[CrossRef\]](#) [\[PubMed\]](#)
- Zhao, X.; Li, X.; Hu, W.; Liu, J.; Di, N.; Duan, J.; Li, D.; Liu, Y.; Guo, Y.; Wang, A.; et al. Long-term variation of the sap flow to tree diameter relation in a temperate poplar forest. *J. Hydrol.* **2023**, *618*, 129189. [\[CrossRef\]](#)
- Oren, R.; Phillips, N.; Ewers, B.E.; Pataki, D.E.; Megonigal, J.P. Sap-flux-scaled transpiration responses to light, vapor pressure deficit, and leaf area reduction in a flooded *Taxodium distichum* forest. *Tree Physiol.* **1999**, *19*, 337–347. [\[CrossRef\]](#) [\[PubMed\]](#)
- Liu, X.Z.; Kang, S.Z.; Li, F.S. Simulation of artificial neural network model for trunk sap flow of *Pyrus pyrifolia* and its comparison with multiple-linear regression. *Agric. Water Manag.* **2009**, *96*, 939–945. [\[CrossRef\]](#)
- Loranty, M.M.; Mackay, D.S.; Ewers, B.E.; Adelman, J.D.; Kruger, E.L. Environmental drivers of spatial variation in whole-tree transpiration in an aspen-dominated upland-to-wetland forest gradient. *Water Resour. Res.* **2008**, *44*, 15. [\[CrossRef\]](#)
- Chang, X.X.; Zhao, W.Z.; He, Z.B. Radial pattern of sap flow and response to microclimate and soil moisture in Qinghai spruce (*Picea crassifolia*) in the upper Heihe River Basin of arid northwestern China. *Agric. For. Meteorol.* **2014**, *187*, 14–21. [\[CrossRef\]](#)
- Chen, X.; Zhao, P.; Hu, Y.T.; Zhao, X.H.; Ouyang, L.; Zhu, L.W.; Ni, G.Y. The sap flow-based assessment of atmospheric trace gas uptake by three forest types in subtropical China on different timescales. *Environ. Sci. Pollut. Res.* **2018**, *25*, 28431–28444. [\[CrossRef\]](#) [\[PubMed\]](#)
- Hayat, M.; Yan, C.H.; Xiang, J.; Xiong, B.W.; Qin, L.J.; Khan, A.; Wang, B.; Khan, M.H.; Zou, Z.D.; Qiu, G.Y. Multiple-Temporal Scale Variations in Nighttime Sap Flow Response to Environmental Factors in *Ficus concinna* over a Subtropical Megacity, Southern China. *Forests* **2022**, *13*, 21. [\[CrossRef\]](#)

23. Kubota, M.; Tenhunen, J.; Zimmermann, R.; Schmidt, M.; Kakubari, Y. Influence of environmental conditions on radial patterns of sap flux density of a 70-year *Fagus crenata* trees in the Naeba Mountains, Japan. *Ann. For. Sci.* **2005**, *62*, 289–296. [[CrossRef](#)]
24. Gazal, R.M.; Scott, R.L.; Goodrich, D.C.; Williams, D.G. Controls on transpiration in a semiarid riparian cottonwood forest. *Agric. For. Meteorol.* **2006**, *137*, 56–67. [[CrossRef](#)]
25. Liu, Z.; Yu, S.; Xu, L.; Wang, Y.; Yu, P.; Chao, Y. Differentiated responses of daytime and nighttime sap flow to soil water deficit in a larch plantation in Northwest China. *Agric. Water Manag.* **2023**, *289*, 108540. [[CrossRef](#)]
26. Bernier, P.Y.; Bartlett, P.; Black, T.A.; Barr, A.; Kljun, N.; McCaughey, J.H. Drought constraints on transpiration and canopy conductance in mature aspen and jack pine stands. *Agric. For. Meteorol.* **2006**, *140*, 64–78. [[CrossRef](#)]
27. MacKay, S.L.; Arain, M.A.; Khomik, M.; Brodeur, J.J.; Schumacher, J.; Hartmann, H.; Peichl, M. The impact of induced drought on transpiration and growth in a temperate pine plantation forest. *Hydrol. Process.* **2012**, *26*, 1779–1791. [[CrossRef](#)]
28. Huang, J.T.; Zhou, Y.X.; Yin, L.H.; Wenninger, J.; Zhang, J.; Hou, G.C.; Zhang, E.Y.; Uhlenbrook, S. Climatic controls on sap flow dynamics and used water sources of *Salix psammophila* in a semi-arid environment in northwest China. *Environ. Earth Sci.* **2015**, *73*, 289–301. [[CrossRef](#)]
29. Fan, Y.; Miguez-Macho, G.; Jobbágy, E.G.; Jackson, R.B.; Otero-Casal, C. Hydrologic regulation of plant rooting depth. *Proc. Natl. Acad. Sci. USA* **2017**, *114*, 10572–10577. [[CrossRef](#)]
30. Petřík, P.; Zavadilová, I.; Sigut, L.; Kowalska, N.; Petek-Petrik, A.; Szatniewska, J.; Jocher, G.; Pavelka, M. Impact of Environmental Conditions and Seasonality on Ecosystem Transpiration and Evapotranspiration Partitioning (T/ET Ratio) of Pure European Beech Forest. *Water* **2022**, *14*, 17. [[CrossRef](#)]
31. Nalevanková, P.; Sitková, Z.; Kucera, J.; Strelcová, K. Impact of Water Deficit on Seasonal and Diurnal Dynamics of European Beech Transpiration and Time-Lag Effect between Stand Transpiration and Environmental Drivers. *Water* **2020**, *12*, 21. [[CrossRef](#)]
32. Oberhuber, W.; Hammerle, A.; Kofler, W. Tree water status and growth of saplings and mature Norway spruce (*Picea abies*) at a dry distribution limit. *Front. Plant Sci.* **2015**, *6*, 703. [[CrossRef](#)] [[PubMed](#)]
33. Zavadilová, I.; Szatniewska, J.; Petrik, P.; Mauer, O.; Pokorný, R.; Stojanović, M. Sap flow and growth response of Norway spruce under long-term partial rainfall exclusion at low altitude. *Front. Plant Sci.* **2023**, *14*, 1089706. [[CrossRef](#)]
34. Xia, G.; Kang, S.; Li, F.; Zhang, J.; Zhou, Q. Diurnal and seasonal variations of sap flow of *Caragana korshinskii* in the arid desert region of north-west China. *Hydrol. Process.* **2008**, *22*, 1197–1205. [[CrossRef](#)]
35. Qian, D.; Zha, T.S.; Jia, X.; Wu, B.; Zhang, Y.Q.; Bourque, C.P.A.; Qin, S.G.; Peltola, H. Adaptive, water-conserving strategies in *Hedysarum mongolicum* endemic to a desert shrubland ecosystem. *Environ. Earth Sci.* **2015**, *74*, 6039–6046. [[CrossRef](#)]
36. Zha, T.S.; Li, C.Y.; Kellomäki, S.; Peltola, H.; Wang, K.Y.; Zhang, Y.Q. Controls of Evapotranspiration and CO₂ Fluxes from Scots Pine by Surface Conductance and Abiotic Factors. *PLoS ONE* **2013**, *8*, 10. [[CrossRef](#)] [[PubMed](#)]
37. Hayat, M.; Zha, T.S.; Jia, X.; Iqbal, S.; Qian, D.; Bourque, C.P.A.; Khan, A.; Tian, Y.; Bai, Y.J.; Liu, P.; et al. A multiple-temporal scale analysis of biophysical control of sap flow in *Salix psammophila* growing in a semiarid shrubland ecosystem of northwest China. *Agric. For. Meteorol.* **2020**, *288*, 12. [[CrossRef](#)]
38. Ma, L.; Lu, P.; Zhao, P.; Rao, X.Q.; Cai, X.A.; Zeng, X.P. Diurnal, daily, seasonal and annual patterns of sap-flux-scaled transpiration from an *Acacia mangium* plantation in South China. *Ann. For. Sci.* **2008**, *65*, 9. [[CrossRef](#)]
39. Ma, F.S.; Kang, S.Z.; Li, F.S.; Zhang, J.H.; Du, T.S.; Hu, X.T.; Wang, M.X. Effect of water deficit in different growth stages on stem sap flux of greenhouse grown pear-jujube tree. *Agric. Water Manag.* **2007**, *90*, 190–196. [[CrossRef](#)]
40. Zhang, J.G.; Guan, J.H.; Shi, W.Y.; Yamanaka, N.; Du, S. Interannual variation in stand transpiration estimated by sap flow measurement in a semi-arid black locust plantation, Loess Plateau, China. *Ecophysiology* **2015**, *8*, 137–147. [[CrossRef](#)]
41. Zheng, H.; Wang, Q.F.; Zhu, X.J.; Li, Y.N.; Yu, G.R. Hysteresis Responses of Evapotranspiration to Meteorological Factors at a Diel Timescale: Patterns and Causes. *PLoS ONE* **2014**, *9*, 10. [[CrossRef](#)] [[PubMed](#)]
42. Chen, Z.; Zhang, Z.; Sun, G.; Chen, L.; Xu, H.; Chen, S. Biophysical controls on nocturnal sap flow in plantation forests in a semi-arid region of northern China. *Agric. For. Meteorol.* **2020**, *284*, 107904. [[CrossRef](#)]
43. Phillips, N.; Oren, R.; Zimmermann, R.; Wright, S.J. Temporal patterns of water flux in trees and lianas in a Panamanian moist forest. *Trees-Struct. Funct.* **1999**, *14*, 116–123. [[CrossRef](#)]
44. Oguntunde, P.G.; van de Giesen, N.C.; Vlek, P.L.G.; Eggers, H. Water Flux in a Cashew Orchard during a Wet-to-Dry Transition Period: Analysis of Sap Flow and Eddy Correlation Measurements. *Earth Interact.* **2004**, *8*, 17. [[CrossRef](#)]
45. Tu, J.; Wei, X.H.; Huang, B.B.; Fan, H.B.; Jian, M.F.; Li, W. Improvement of sap flow estimation by including phenological index and time-lag effect in back-propagation neural network models. *Agric. For. Meteorol.* **2019**, *276*, 7. [[CrossRef](#)]
46. Ma, T.; Wang, T.; Yang, D.; Yang, S. Impacts of vegetation restoration on water resources and carbon sequestration in the mountainous area of Haihe River basin, China. *Sci. Total Environ.* **2023**, *869*, 161724. [[CrossRef](#)] [[PubMed](#)]
47. Lei, H.; Yang, D.; Huang, M. Impacts of climate change and vegetation dynamics on runoff in the mountainous region of the Haihe River basin in the past five decades. *J. Hydrol.* **2014**, *511*, 786–799. [[CrossRef](#)]
48. Tie, Q.; Hu, H.C.; Tian, F.Q.; Guan, H.D.; Lin, H. Environmental and physiological controls on sap flow in a subhumid mountainous catchment in North China. *Agric. For. Meteorol.* **2017**, *240*, 46–57. [[CrossRef](#)]
49. Wang, Q.M.; Jiang, S.; Zhai, J.Q.; He, G.H.; Zhao, Y.; Zhu, Y.N.; He, X.; Li, H.H.; Wang, L.Z.; He, F.; et al. Effects of vegetation restoration on evapotranspiration water consumption in mountainous areas and assessment of its remaining restoration space. *J. Hydrol.* **2022**, *605*, 12. [[CrossRef](#)]

50. Peng, H.; Jia, Y.W.; Zhan, C.S.; Xu, W.H. Topographic controls on ecosystem evapotranspiration and net primary productivity under climate warming in the Taihang Mountains, China. *J. Hydrol.* **2020**, *581*, 9. [[CrossRef](#)]
51. Ji, S.; Ren, S.; Li, Y.; Dong, J.; Wang, L.; Quan, Q.; Liu, J. Diverse responses of spring phenology to pre-season drought and warming under different biomes in the North China Plain. *Sci Total Env.* **2021**, *766*, 144437. [[CrossRef](#)]
52. Xiao-Qiu, C.Y.-Z.L.W.-G.C. Process-based simulation of autumn phenology of trees and the regional differentiation attribution in northern China. *Chin. J. Plant Ecol.* **2022**, *46*, 753–765. [[CrossRef](#)]
53. Fuchs, S.; Leuschner, C.; Link, R.; Coners, H.; Schuldt, B. Calibration and comparison of thermal dissipation, heat ratio and heat field deformation sap flow probes for diffuse-porous trees. *Agric. For. Meteorol.* **2017**, *244–245*, 151–161. [[CrossRef](#)]
54. Flo, V.; Martinez-Vilalta, J.; Steppe, K.; Schuldt, B.; Poyatos, R. A synthesis of bias and uncertainty in sap flow methods. *Agric. For. Meteorol.* **2019**, *271*, 362–374. [[CrossRef](#)]
55. Tong, Y.Q.; Liu, J.; Han, X.; Zhang, T.; Dong, Y.H.; Wu, M.G.; Qin, S.J.; Wei, Y.W.; Chen, Z.J.; Zhou, Y.B. Radial and seasonal variation of sap flow and its response to meteorological factors in sandy *Pinus sylvestris* var. *mongolica* plantations in the Three North Shelterbelt of China. *Agric. For. Meteorol.* **2023**, *328*, 9. [[CrossRef](#)]
56. Du, S.; Wang, Y.L.; Kume, T.; Zhang, J.G.; Otsuki, K.; Yamanaka, N.; Liu, G.B. Sapflow characteristics and climatic responses in three forest species in the semiarid Loess Plateau region of China. *Agric. For. Meteorol.* **2011**, *151*, 1–10. [[CrossRef](#)]
57. Liu, C.W.; Du, T.S.; Li, F.S.; Kang, S.Z.; Li, S.E.; Tong, L. Trunk sap flow characteristics during two growth stages of apple tree and its relationships with affecting factors in an arid region of northwest China. *Agric. Water Manag.* **2012**, *104*, 193–202. [[CrossRef](#)]
58. Xu, X.Y.; Tong, L.; Li, F.S.; Kang, S.Z.; Qu, Y.P. Sap flow of irrigated *Populus alba* var. *pyramidalis* and its relationship with environmental factors and leaf area index in an arid region of Northwest China. *J. For. Res.* **2011**, *16*, 144–152. [[CrossRef](#)]
59. Chuang, Y.L.; Oren, R.; Bertozzi, A.L.; Phillips, N.; Katul, G.G. The porous media model for the hydraulic system of a conifer tree: Linking sap flux data to transpiration rate. *Ecol. Model.* **2006**, *191*, 447–468. [[CrossRef](#)]
60. Huang, L.; Zhang, Z.S.; Li, X.R. Sap flow of *Artemisia ordosica* and the influence of environmental factors in a revegetated desert area: Tengger Desert, China. *Hydrol. Process.* **2010**, *24*, 1248–1253. [[CrossRef](#)]
61. Han, C.; Chen, N.; Zhang, C.K.; Liu, Y.J.; Khan, S.; Lu, K.L.; Li, Y.G.; Dong, X.X.; Zhao, C.M. Sap flow and responses to meteorological about the *Larix principis-rupprechtii* plantation in Gansu Xinlong mountain, northwestern China. *For. Ecol. Manag.* **2019**, *451*, 9. [[CrossRef](#)]
62. Horna, V.; Schuldt, B.; Brix, S.; Leuschner, C. Environment and tree size controlling stem sap flux in a perhumid tropical forest of Central Sulawesi, Indonesia. *Ann. For. Sci.* **2011**, *68*, 1027–1038. [[CrossRef](#)]
63. Kume, T.; Takizawa, H.; Yoshifuji, N.; Tanaka, K.; Tantasirin, C.; Tanaka, N.; Suzuki, M. Impact of soil drought on sap flow and water status of evergreen trees in a tropical monsoon forest in northern Thailand. *For. Ecol. Manag.* **2007**, *238*, 220–230. [[CrossRef](#)]
64. Meinzer, F.C.; Andrade, J.L.; Goldstein, G.; Holbrook, N.M.; Cavelier, J.; Wright, S.J. Partitioning of soil water among canopy trees in a seasonally dry tropical forest. *Oecologia* **1999**, *121*, 293–301. [[CrossRef](#)]
65. Bovard, B.D.; Curtis, P.S.; Vogel, C.S.; Su, H.B.; Schmid, H.P. Environmental controls on sap flow in a northern hardwood forest. *Tree Physiol.* **2005**, *25*, 31–38. [[CrossRef](#)]
66. Guo, W.H.; Li, B.; Zhang, X.S.; Wang, R.Q. Effects of water stress on water use efficiency and water balance components of *Hippophae rhamnoides* and *Caragana intermedia* in the soil-plant-atmosphere continuum. *Agrofor. Syst.* **2010**, *80*, 423–435. [[CrossRef](#)]
67. Wang, X.Z.; Zhang, W.H.; Miao, Y.X.; Gao, L.H. Root-Zone Warming Differently Benefits Mature and Newly Unfolded Leaves of *Cucumis sativus* L. Seedlings under Sub-Optimal Temperature Stress. *PLoS ONE* **2016**, *11*, 20. [[CrossRef](#)] [[PubMed](#)]
68. Lee, S.H.; Chung, G.C.; Jang, J.Y.; Ahn, S.J.; Zwiazek, J.J. Overexpression of PIP2;5 Aquaporin Alleviates Effects of Low Root Temperature on Cell Hydraulic Conductivity and Growth in Arabidopsis (vol 159, pg 479, 2012). *Plant Physiol.* **2012**, *159*, 1291. [[CrossRef](#)] [[PubMed](#)]
69. Lee, S.H.; Chung, G.C. Sensitivity of root system to low temperature appears to be associated with the root hydraulic properties through aquaporin activity. *Sci. Hort.* **2005**, *105*, 1–11. [[CrossRef](#)]
70. Xia, Z.Q.; Zhang, G.X.; Zhang, S.B.; Wang, Q.; Fu, Y.F.; Lu, H.D. Efficacy of Root Zone Temperature Increase in Root and Shoot Development and Hormone Changes in Different Maize Genotypes. *Agriculture* **2021**, *11*, 13. [[CrossRef](#)]
71. Wang, H.L.; Tetzlaff, D.; Soulsby, C. Hysteretic response of sap flow in Scots pine (*Pinus sylvestris*) to meteorological forcing in a humid low-energy headwater catchment. *Ecohydrology* **2019**, *12*, 11. [[CrossRef](#)]
72. Zha, T.S.; Qian, D.; Jia, X.; Bai, Y.J.; Tian, Y.; Bourque, C.P.A.; Ma, J.Y.; Feng, W.; Wu, B.; Peltola, H. Soil moisture control of sap-flow response to biophysical factors in a desert-shrub species, *Artemisia ordosica*. *Biogeosciences* **2017**, *14*, 4533–4544. [[CrossRef](#)]
73. Zhang, Q.; Manzoni, S.; Katul, G.; Porporato, A.; Yang, D.W. The hysteretic evapotranspiration—Vapor pressure deficit relation. *J. Geophys. Res. Biogeosci.* **2014**, *119*, 125–140. [[CrossRef](#)]
74. O’Grady, A.P.; Eamus, D.; Hutley, L.B. Transpiration increases during the dry season: Patterns of tree water use in eucalypt open-forests of northern Australia. *Tree Physiol.* **1999**, *19*, 591–597. [[CrossRef](#)] [[PubMed](#)]
75. Kume, T.; Komatsu, H.; Kuraji, K.; Suzuki, M. Less than 20-min time lags between transpiration and stem sap flow in emergent trees in a Bornean tropical rainforest. *Agric. For. Meteorol.* **2008**, *148*, 1181–1189. [[CrossRef](#)]
76. Tsuruta, K.; Kume, T.; Komatsu, H.; Otsuki, K. Effects of soil water decline on diurnal and seasonal variations in sap flux density for differently aged Japanese cypress (*Chamaecyparis obtusa*) trees. *Ann. For. Res.* **2018**, *61*, 5–18. [[CrossRef](#)]
77. Wan, L.; Zhang, Q.; Cheng, L.; Liu, Y.; Qin, S.; Xu, J.; Wang, Y. What determines the time lags of sap flux with solar radiation and vapor pressure deficit? *Agric. For. Meteorol.* **2023**, *333*, 109414. [[CrossRef](#)]

78. O'Brien, J.J.; Oberbauer, S.F.; Clark, D.B. Whole tree xylem sap flow responses to multiple environmental variables in a wet tropical forest. *Plant Cell Environ.* **2004**, *27*, 551–567. [[CrossRef](#)]
79. Matheny, A.M.; Bohrer, G.; Vogel, C.S.; Morin, T.H.; He, L.L.; Frasson, R.P.D.; Mirfenderesgi, G.; Schäfer, K.V.R.; Gough, C.M.; Ivanov, V.Y.; et al. Species-specific transpiration responses to intermediate disturbance in a northern hardwood forest. *J. Geophys. Res. Biogeosci.* **2014**, *119*, 2292–2311. [[CrossRef](#)]

Disclaimer/Publisher's Note: The statements, opinions and data contained in all publications are solely those of the individual author(s) and contributor(s) and not of MDPI and/or the editor(s). MDPI and/or the editor(s) disclaim responsibility for any injury to people or property resulting from any ideas, methods, instructions or products referred to in the content.